

Evaluating Sample Utility for Efficient Data Selection by Mimicking Model Weights

Tzu-Heng Huang^{*1} Manjot Bilkhu^{†2} John Cooper¹ Frederic Sala¹
Javier Movellan²

¹University of Wisconsin-Madison

²Apple Inc.

¹{thuang273, jfcooper2, fredsalas}@wisc.edu
²{mbilkhu, movellan}@apple.com

June 16, 2025

Abstract


Multimodal models are trained on large-scale web-crawled datasets, which often contain noise, bias, and irrelevant information. This motivates the use of data selection techniques, which can be divided into model-free variants, relying on heuristic rules and downstream datasets, and model-based approaches, such as those using influence functions. The former can be expensive to design and risks introducing unwanted dataset dependencies, while the latter are often computationally prohibitive. In this work, we propose an efficient, model-based approach using the **Mimic Score**, a new data-quality metric that leverages the weights of a reference model to assess the usefulness of individual samples for training a new model. Our method relies on measuring alignments between training gradients and a target direction induced by this reference model. Building on the derived mimic scores, we develop **Grad-Mimic**: a framework that prioritizes samples to learn, estimates overall sample utility, and creates effective filters. Empirically, using mimic scores to guide training improves data efficiency, accelerates convergence, yields consistent performance gains across six image datasets, and enhances CLIP models with **20.7% fewer training steps**. Moreover, mimic score-based filters complement existing filtering methods, e.g., training improved CLIP models with **4.7 million fewer samples** while offering accurate estimation of dataset quality.

1 Introduction

Large-scale web-crawled datasets are fundamental to the success of modern multimodal models such as AIMv2 [1], ALIGN [2], OpenAI CLIP [3], and SigLIP [4]. These datasets provide vast quantities of information—but inevitably contain noise, biases, and irrelevant content. To mitigate these, data selection—ruling out undesirable samples—has emerged as a critical step in the development pipeline [5, 6]. For example, the FineWeb dataset [7], containing 15 trillion text tokens, undergoes eight carefully designed filtering steps to ensure high model performance.

Current selection strategies; however, are far from satisfactory. We can broadly divide them into two categories: model-free methods, such as those based on handcrafted heuristics or semantic similarity to downstream datasets [8, 9] often *require costly trial-and-error* to establish selection rules and *add unwanted dependencies* on other datasets. These methods also lack the granularity needed to assess individual utility, leading to suboptimal training outcomes. In contrast, model-based techniques, such as those building specialized filtering networks [10, 11, 12, 13], scoring samples through a pretrained reference model’s loss [14, 15], or using influence functions [16, 17, 18, 19, 20], *increase the complexity* of the pipeline and are often *computationally expensive*. These shortcomings motivate the need for a *simpler, dataset-agnostic, compute-efficient* way to curate high-quality datasets.

We introduce the **Mimic Score**, a new data-quality metric that quantifies each training sample’s contribution to effective weight updates. We argue that samples whose gradients potentially pull the model in undesirable directions—and thus misguide weight updates—should be down-weighted or discarded. To establish a desirable weight update, we leverage the direction pointing toward the weights of a pretrained reference model¹, located in a

^{*}  Work done during an internship at Apple.

[†] Corresponding author. Email: mbilkhu@apple.com & thuang273@wisc.edu.

¹Note that our goal is to *select high-quality data*, not to reproduce the reference model. While insight into reference model’s training data would be valuable, we assume it is inaccessible—a common situation with many modern open-source models.

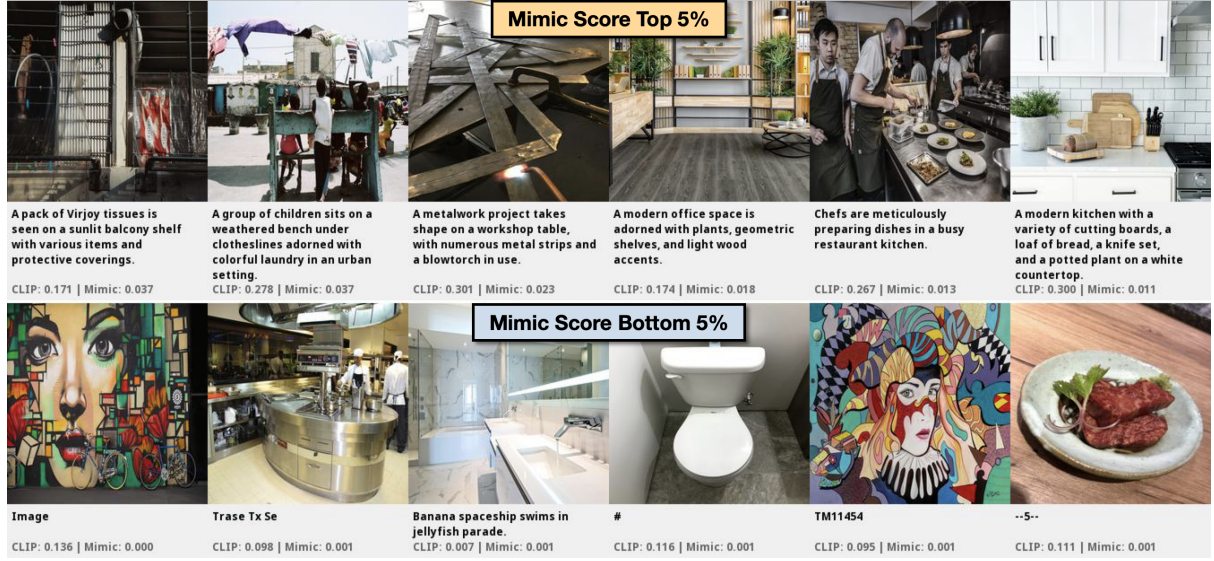


Figure 1: **High-value vs. low-value samples identified by the Mimic score:** Randomly selected samples from the top 5% (first row) and bottom 5% (second row) of web-crawled data, ranked by their mimic scores. Each image includes its caption and CLIP score (higher indicates better quality). Mimic scores align closely with CLIP scores. High-value samples generally have detailed captions and coherent visuals, while low-value ones carry short captions and misaligned content.

more optimal part of the weight space, as *our proxy*. The mimic score is computed for each sample by measuring the alignment between its negative gradient and the direction induced by this reference model. A high alignment score indicates a sample can steer the model toward this preferred region, while a low one would divert the model.

Using model weights to evaluate sample utility offers multiple practical benefits. First, the growing supply of well-trained models makes this approach more accessible than ever. Second, unlike methods that derive selection guides using the gradients on noise-free validation datasets [18, 19, 20], mimic score *avoids extra validation computations, bypassing the difficulties of curating such dataset and ensuring its quality*. Finally, many reference model-based techniques compute excess loss through additional full inference [14, 15]. Our mechanism instead is a much simpler operation based on the discrepancy of model weights, which *can substantially reduce compute overheads*.

Building on the mimic score, we develop **Grad-Mimic**, a two-stage data-selection framework:

- **Online Batch Re-weighting.** During training, Grad-Mimic computes mimic scores on the fly and prioritizes samples to learn, enhancing data efficiency and accelerating convergence.
- **Offline Sample Selection.** After training, Grad-Mimic aggregates sample’s mimic scores across training steps to estimate an overall sample utility. Such combined estimate serves as a reliable filter, enabling the construction of a smaller, higher-quality dataset for future use.

We validate the capabilities of Grad-mimic in a broad range of scenarios. For ***mislabeled sample detection***, we show in a controlled setting, Grad-Mimic accurately identifies noisy labels and estimates overall dataset quality. By down-weighting undesirable samples during training, it enhances data efficiency and model performance across six image datasets. For ***large-scale data curation***, we scale our testbed to web-crawled multimodal data by training CLIP models from scratch [3] on 10M and 100M samples [21]. Using publicly released pretrained weights as our reference, mimic scores effectively navigate training, **reducing 20.7% training steps** to convergence. The resulting filter outperforms human-designed ones and complements CLIP score-based filters [22], lifting CLIP model performance with **4.7M fewer training samples**.

We summarize our contributions as follows:

- **New Data-quality Metric:** We introduce Mimic Score to assess sample utility by measuring the alignment between training gradients and a vector toward the reference model in the weight space.
- **Efficient Data Selection Framework:** Built on Mimic Score, we present Grad-Mimic, a framework that efficiently prioritizes valuable samples to learn, enhances data efficiency, accelerates convergence, and automates effective data selection.

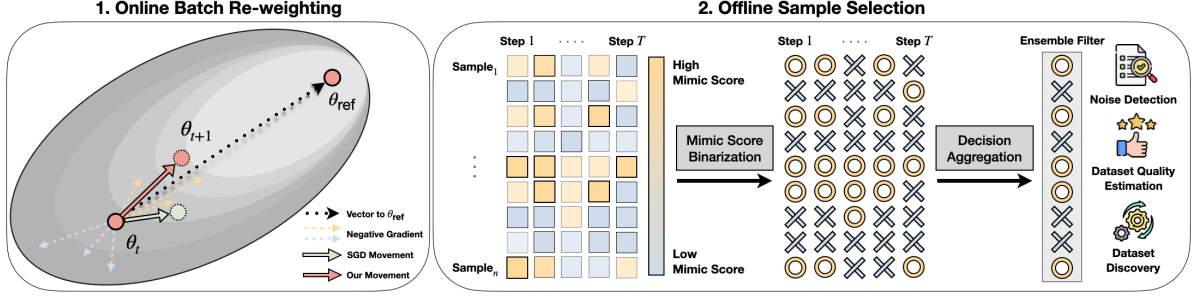


Figure 2: **Grad-Mimic Two-stage Workflow**: During training, Grad-Mimic measures alignments using the vector toward the reference model’s weight space against each sample’s negative gradient. It then adapts alignment scores to re-weight gradients for weight updates. After training, the derived alignment scores, mimic scores, are used to identify low-value samples and build an ensemble filter, which can be used for *noise detection*, *dataset quality assessment*, and *training dataset discovery*.

- **Dataset Quality Assessment**: Mimic Score, along with its ensemble filters, provides reliable estimates of dataset quality and model performance gains and improves existing filtering strategies.

2 Related Work

Our work explores using the weights of a reference model to evaluate sample utility, intersecting three key areas: (i) data selection, (ii) data curation for multimodal models, and (iii) weak supervision.

Data Selection. Data selection techniques can be categorized into group- and sample-level approaches. Group-level approaches focus on optimizing data domain mixtures to curate high-quality datasets [23, 24, 25, 26]. Sample-level methods, which are the focus of Grad-Mimic, aim to provide a score measuring sample utility and rule out undesired samples. Prior research has explored various gradient-based strategies, such as identifying impactful samples through gradient magnitudes [27], analyzing gradient similarities to other training batches [28], selecting key samples that can capture full training [29, 30], and using gradients computed on noisy-free validation sets [18, 19, 20]. These methods; however, are sensitive to noisy batch gradients and often incur extra computation. Grad-Mimic sidesteps both issues *with the help of a reference model*.

Data Curation for Multimodal Models. Multimodal models rely on large-scale web datasets [31, 21, 32]; however, quantity comes at a price: unconstrained crawling amplifies noise and requires careful curation. Previous approaches have included selecting samples based on semantic similarity to the downstream evaluation datasets [8, 9], using semantic deduplication [33], developing specialized filtering networks [10, 11, 12, 13], and using data influence functions [16, 17]. While effective, they require access to other datasets, introduce training complexities, or demand substantial compute. Grad-Mimic offers a more efficient alternative: *using public available models and the discrepancy in model weights to identify useful samples*.

Weak Supervision. Weak supervision is a framework to construct labeled datasets by combining multiple noisy label estimates [34, 35, 36, 37]. These estimates can come from sources such as heuristic labeling rules, domain knowledge, or pretrained models [38, 39], often encoded as labeling functions. Labeling functions’ outputs are modeled and aggregated to produce probabilistic labeling decisions [34]. Weak supervision has demonstrated success in diverse domains [40, 41, 42, 43, 44]. Most prior works focus on weak label aggregation to construct datasets. Grad-Mimic leverages it for a new purpose: *modeling each sample’s utility assessments for a combined filtering decision*.

3 Evaluating Sample Utility

Our goal is to quantify training sample contributions to learning process when we (i) have a model to be trained and (ii) access a pretrained reference model as proxy. Our principle is that *samples that potentially pull the model in an undesirable direction, thereby misdirecting weight updates, should be considered low-value*. We start with setup and notation, then explain how an intermediate scoring metric is derived and used inside our data selection framework, Grad-Mimic (Sec. 4).

Notation. Let $D = \{s_i\}_{i=1}^n$ denote a dataset of n samples drawn from a distribution \mathcal{D} supported on the space \mathcal{S} . At training step t , model parameters θ_t , are iteratively optimized using the dataset D . While our framework supports various training settings, we focus on supervised learning for clarity. We assume $\mathcal{S} = \mathcal{X} \times \mathcal{Y}$, where \mathcal{X} is the input space and \mathcal{Y} is the label space. Each sample s_i can be expressed as (x_i, y_i) , where noise may be present either in the instance x_i or in the label y_i . The empirical loss across all the samples is defined as $\frac{1}{n} \sum_{i=1}^n \ell(x_i, y_i)$, and each sample’s gradient with respect to the model parameters θ_t is written as: $g_{i,t} := \nabla_{\theta_t} \ell(x_i, y_i)$. A standard update to model parameters is $\theta_{t+1} := \theta_t - \eta \frac{1}{b} \sum_{i=1}^b g_{i,t}$, where η is the learning rate and b is the batch size.

Mimic Score Calculation. To evaluate whether a sample’s gradient pulls the model in an undesirable direction, we use the weights of a pretrained reference model as our proxy guide. These reference weights, denoted by θ_{ref} , are assumed reside in a more optimal part of the weight space, such that $\ell(\theta_{\text{ref}}) < \ell(\theta_t)$. We use the vector from the current model’s weight space θ_t to θ_{ref} to measure each sample utility in approximating a better weight configuration (θ_{ref}). These weights can be layer-specific, e.g., model weights in the last layer, which usually store more informative features [45, 46].

Reference weights can be obtained either by training a model on a (hold-out) dataset until it meets the desired performance [15, 14], if resource permits, or, more efficiently, by using an existing well-trained public model, which sidesteps both data-access constraints and costly training.

The vector pointing toward reference model’s weights, at training step t , is represented by $v_t := \theta_{\text{ref}} - \theta_t$. We examine how each sample’s negative gradient $-g_{i,t}$, intended for updating model weights, aligns with vector v_t . We measure this alignment degree by considering both the direction and magnitude of the negative gradient. Specifically, we compute the projection length of $-g_{i,t}$ onto v_t , yielding an alignment score $m_{i,t}$, computed as follows

$$\text{mimic_score}(s_{i,t}) := m_{i,t} = \frac{\langle -g_{i,t}, v_t \rangle}{\|v_t\|}. \quad (1)$$

This alignment score, named *mimic score*, reflects **how much a sample can drive the model closer to a preferred weight space**. A sample having a lower mimic score suggests it has limited utility in guiding effective weight updates, making it a potential candidate for exclusion from future training.

4 Data Selection Framework

Building on this simple data-quality metric, we package it into Grad-Mimic, a two-stage data selection framework that first *prioritizes which samples to learn* (Sec. 4.1) and then *combines sample utilities* to design an *effective ensemble data filter* (Sec. 4.2). A complete Grad-Mimic workflow is in Fig. 2.

4.1 Stage 1: Online Batch Re-weighting.

We first use mimic scores to aid model training through improving data efficiency by *re-weighting*. Unlike gradient descent, which assigns uniform weight to mini-batch samples, Grad-Mimic computes mimic scores on the fly to amplify helpful samples and down-weight unhelpful ones.

To achieve this, each sample’s mimic score is first normalized using the softmax function with a temperature parameter, τ . The normalized score for a sample s_i in a batch of size b is computed as

$$\bar{m}_{i,t} = \frac{e^{m_{i,t}/\tau}}{\sum_{j=1}^b e^{m_{j,t}/\tau}}. \quad (2)$$

Then, the weight update step in Grad-Mimic is modified as

$$\theta_{t+1} := \theta_t - \eta \sum_{i=1}^b \bar{m}_{i,t} \cdot g_{i,t}. \quad (3)$$

The temperature τ controls the sensitivity of sample reweighting, allowing us to adjust how sharply the model prioritizes samples. A lower temperature results in a more aggressive focus on learning the most aligned samples, while a higher one encourages Grad-Mimic converges to gradient descent.

Theoretical Analysis. We provide an analysis for *effective batch reweighting* in Appendix A. In particular, we study conditions where Grad-Mimic converges faster than standard gradient descent.

4.2 Stage 2: Offline Sample Selection.

The second stage of Grad-Mimic converts computed mimic scores, estimated sample utilities, into a unified assessment, enabling us to curate a higher-quality training dataset with developed data filter.

Mimic Score Binarization. Grad-Mimic first gathers normalized mimic scores for each sample at every training step. These indicate their intermediate contributions to learning. We convert continuous scores into *binary retain/discard decisions* and explore three schemes:

- *Threshold-based:* A sample is chosen if its mimic score exceeds a defined threshold. A natural choice can be set as $1/b$ (indicating greater than uniform).
- *1D Clustering:* Samples are categorized into two groups using clustering (e.g., k -means [47] or Gaussian mixture), allowing unsupervised identification based on their assigned clusters.
- *Top- k Percent:* Samples are ranked by their mimic score, and the top- k percent are chosen. The value of k can be adjusted based on the available training budget.

Decision Aggregation. A filtering decision made at a single step can be noisy and ignore training dynamics. To address this, we treat each step’s binarized assessments as weak votes and use *weak supervision techniques* [34, 35, 36, 37] to combine filtering decisions across training steps. We start by learning a generative model to estimate the reliability of each step’s assessments [36]. Once established, this model produces probabilistic aggregated decisions. This consensus mitigates assessment noise and captures how a sample’s utility evolves. Empirically, we employ the aggregation step from Snorkel framework [35], a widely-used method in the weak supervision community.

Ultimately, the ensemble filtering decisions yield a curated subset that can be reused in later training runs. Moreover, we can use their statistics to estimate training dataset quality by either analyzing *retention rate* (fraction of samples retained) or *averaged mimic score*. We discuss weak supervision setups and summarize algorithms in both online and offline stages in Appendix B.

5 Experiments

We validate Grad-Mimic’s effectiveness using two experimental setups across diverse scales and domains. First, we test in a controlled setting, adding noise sample labels (Sec. 5.1), then evaluate on large-scale web-crawled datasets (Sec. 5.2). Our goals are to confirm key claims in both settings:

- **Enhanced Data Efficiency:** The weights of pretrained reference model serve as reliable guide. Using derived mimic scores to prioritize samples improves data efficiency and speed up convergence.
- **Accurate Sample Identification:** Grad-Mimic precisely detects noisy samples, constructs effective ensemble filter, and automates data selection for high-quality datasets.
- **Dataset Quality Assessment:** Mimic scores and their resulting filters provide reliable estimates of dataset quality and predict model performance gains.

5.1 Simulating Misabeled Samples

Setups. We begin with a controlled experiment by adding various levels of label noise to six image classification datasets. They are DTD [48], Flowers102 [49], STL10 [50], OxfordIIIT Pet [51], CIFAR10, and CIFAR100 [52]. We fine-tune the ViT-B/16 model [53] on these noisy datasets under two configurations: linear probing, where only the final layer is tuned, and full fine-tuning, where gradients of all model parameters are reweighted based on mimic scores to maximize the impact of useful samples. We normalize mimic scores with a temperature of 0.5 and use a batch size of 32. We simulate pretrained reference models by training ViT-B/16 models on the noise-free version of each dataset and use the last-layer weights as our reference to navigate training on the noisy datasets. We detail more training configurations in Appendix C.

After training, we binarize samples’ mimic scores in two ways: setting one over batch size ($1/b$) as our threshold and using k -means and GMM to cluster. Then we aggregate filter outputs across training steps using Snorkel framework [35].

Expected Results. We aim to validate that a pretrained reference model’s weights can serve as a reliable selection guide, and we expect mimic scores can help identify low-value, mislabeled samples.

Full Fine-tuning	DTD			Flowers102			STL10			Oxford-IIIT Pet			CIFAR10			CIFAR100			Average		
Noise Level	0.4	0.5	0.6	0.4	0.5	0.6	0.4	0.5	0.6	0.4	0.5	0.6	0.4	0.5	0.6	0.4	0.5	0.6	0.4	0.5	0.6
Mini-batch SGD	46.91	42.02	33.24	65.54	55.90	39.84	75.35	58.57	49.98	70.43	64.62	55.63	90.31	86.69	82.01	69.42	63.77	59.28	69.66	61.93	53.33
GraNd	29.73	8.83	15.43	10.80	2.78	27.92	78.39	52.32	64.30	56.83	45.38	45.43	87.56	83.79	80.04	18.65	8.83	7.84	46.99	33.66	40.16
AGRA	46.28	37.29	32.39	0.62	0.93	0.82	84.35	79.94	78.17	76.97	77.11	69.39	89.23	86.79	68.09	11.96	8.44	6.88	51.57	48.42	42.62
Grad-Match	48.88	42.66	33.24	37.92	54.94	42.62	83.86	81.16	77.18	74.35	61.73	51.16	44.48	35.69	37.59	69.41	66.21	20.09	58.82	57.07	43.65
Grad-Mimic	49.20	42.82	33.83	68.58	56.46	44.27	72.06	71.85	83.09	81.98	78.30	73.34	90.52	89.07	66.41	73.97	74.31	24.02	72.72	68.60	54.16

Linear Probing	DTD			Flowers102			STL10			Oxford-IIIT Pet			CIFAR10			CIFAR100			Average		
Noise Level	0.4	0.5	0.6	0.4	0.5	0.6	0.4	0.5	0.6	0.4	0.5	0.6	0.4	0.5	0.6	0.4	0.5	0.6	0.4	0.5	0.6
Mini-batch SGD	51.91	47.71	44.44	28.64	21.50	15.43	96.26	95.49	93.56	87.33	85.55	83.51	92.86	92.14	91.19	75.56	74.38	73.25	72.09	69.46	66.40
GraNd	36.22	30.59	25.32	18.23	13.90	10.49	68.70	59.55	49.68	69.47	60.02	48.13	88.02	85.61	81.48	71.60	70.51	69.27	58.71	53.36	47.40
AGRA	41.81	36.28	31.49	41.81	36.28	31.49	96.19	95.15	93.11	85.25	82.53	78.39	92.51	92.01	90.99	72.50	71.30	69.69	71.68	68.93	65.86
Grad-Match	51.81	47.55	41.33	27.00	20.21	14.90	96.06	95.34	93.44	86.86	85.75	83.18	92.62	92.04	91.17	75.39	74.46	73.18	71.62	69.23	66.20
Grad-Mimic	54.68	54.10	50.43	42.75	37.10	31.71	97.16	97.00	96.90	88.80	88.25	87.14	94.15	93.92	93.80	77.24	76.82	76.05	75.80	74.53	73.01

Table 1: **Stage 1 Results in Simulation Experiment:** Using mimic scores can effectively down-weight mislabeled samples during training, improving data efficiency and denoising capability.

	DTD			Flowers102			STL10			Oxford-IIIT Pet			CIFAR10			CIFAR100					
Noise Level	0.4	0.5	0.6	0.4	0.5	0.6	0.4	0.5	0.6	0.4	0.5	0.6	0.4	0.5	0.6	0.4	0.5	0.6	0.4	0.5	0.6
Threshold (1/32)	85.13	88.91	91.82	90.93	94.9	96.92	90.31	94.11	97.21	94.41	96.86	97.93	98.37	98.19	97.19	97.66	97.57	95.80			
1D k -means	77.13	76.68	77.17	84.45	87.62	87.47	78.90	83.04	78.82	95.80	95.49	93.73	98.62	98.17	97.56	98.10	97.46	96.62			
GMM	97.85	96.72	95.68	98.39	96.96	94.21	97.96	97.16	95.69	98.04	97.07	95.86	95.70	92.89	88.62	95.86	94.31	92.55			

Table 2: **Stage 2 Results in Simulation Experiment:** We report detection results using F1-score. Grad-Mimic reliably detects mislabeled samples across datasets and binarization methods, maintaining strong performance despite varying noise levels.

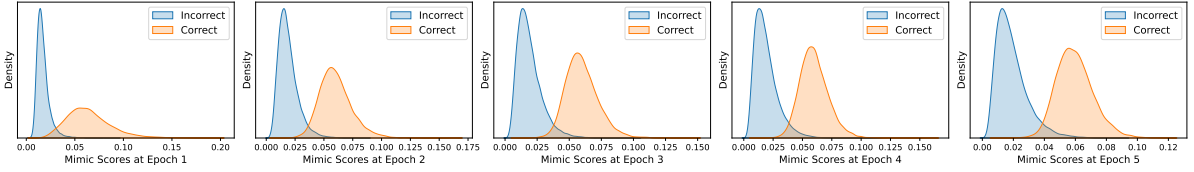


Figure 3: **Mimic Score Distribution:** Extracted from CIFAR100 dataset with a noise level of 0.5. The distributions clearly separate, aligning with the correctness of the labels.

Baselines. We compare Grad-Mimic’s Stage 1 online method with other approaches that use gradient information for sample prioritization. We consider: (i) *Mini-batch SGD*, the standard method, updates weights by averaging gradients within the mini-batch. (ii) *GraNd* [27] reweights samples based on their gradient norm, prioritizing data that induce greater changes. (iii) *AGRA* [28] computes the cosine similarity of each sample gradient to an average gradient of another random batch, then excludes outlier samples. (iv) *Grad-Match* [29] adapts gradients by solving a subset selection problem to identify key samples within each batch.

Furthermore, we compare Grad-Mimic with *Rho-Loss* [14], a reference model-based approach that prioritizes training on worth learning samples, as well as *approximated influence function-based methods*. Results are presented in Appendix D. *Grad-Mimic outperforms both techniques while additionally offering efficiency advantages* (See Appendix E).

Stage 1 Results. We present Grad-Mimic’s two-stage results separately. Stage 1 results, shown in Table 1, report testing accuracy across various methods and noisy datasets using both training configurations. These results demonstrate that Grad-Mimic effectively identifies and down-weights mislabeled samples during training, *enhancing denoising capability*. Notably, in the full fine-tuning setup—where we *only target the last layer to mimic*—Grad-Mimic successfully guides weight updates for the entire model, ultimately outperforming other baseline methods. Beyond denoising improvements, Grad-Mimic enjoys many efficiency benefits than others, *including faster convergence, lower compute runtime, and reduced GPU memory usage*. We place these analysis in Appendix E. Additionally, we explore the impact of reference model quality in Appendix F, further strengthening our approach. These findings all validate the idea that *using the direction induced by a better-performing model can guide model training and improve data efficiency*.

Stage 2 Results. Next, we demonstrate Grad-Mimic’s capability to detect mislabeled samples. We use F1-scores to report the detection results in Table 2. Grad-Mimic accurately identifies mislabeled data across datasets and remains robust when facing different noise levels.

Scale	Training Method	Mimic Layer θ_{ref}	Temperature τ	ImageNet	ImageNet dis. shifts	VTAB	Retrieval	Average over 38 datasets (\uparrow)
Small	Vanilla Training	—	—	0.026	0.035	0.139	0.114	0.131
	Grad-Mimic	Last MLP Layer in Text Encoder	0.05	0.026	0.035	0.147	0.114	0.135
			0.5	0.027	0.035	0.152	0.114	0.139
		Last MLP Layer in Image Encoder	0.05	0.026	0.037	0.162	0.118	0.146
			0.5	0.027	0.035	0.160	0.117	0.145
Medium	Vanilla Training	—	—	0.171	0.148	0.253	0.217	0.254
	Grad-Mimic	Last MLP Layer in Image Encoder	0.05	0.169	0.151	0.262	0.216	0.258

Table 3: **Stage 1 Results in DataComp Experiment:** On both dataset scales, with the aid of publicly available pretrained weights, Grad-Mimic yields higher CLIP model performance. Full table with various temperature settings is placed in Table 8 in Appendix F.

We use CIFAR100 dataset as an example and visualize computed mimic score distribution at each training step in Figure 3. In this dataset, half of the labels are flipped. We can see their distributions clearly separate into two groups, confirming that mimic scores are informative signals to identify samples. Despite variations over training, these dynamics can be captured in our aggregation step.

We use the ensemble filter from each dataset created by GMM clustering to estimate training dataset quality using the proportion of retained data. The results, displayed in Figure 4 (middle), *highly correspond to the presence of label noise*, with a Pearson correlation of **-0.903**. These demonstrate mimic score’s effectiveness for dataset quality estimation.

5.2 Data Selection in Large-scale Web Datasets

Setups. Next, we test Grad-Mimic in a more challenging setting using million-scale web-crawled datasets. We use the small-scale and medium-scale DataComp datasets [21], which contain approximately 10 million and 100 million image-caption pairs², respectively, to train CLIP model from scratch [3]. In these datasets, noise is *naturally* presented in the data. We follow the training setup from DataComp [54, 21] and use publicly available pretrained CLIP model’s weights as our reference³. This reference model, trained on the DataComp-1B dataset (1.4 billion samples), represents the best-performing model accessible to us. It serves as a proxy for the ideal reference point for scenarios where training such powerful models is infeasible. We use the final MLP layer in the text and image encoders respectively as our target to mimic. We evaluate the performance of resulting model using DataComp benchmark, which includes 38 diverse image classification and retrieval tasks. Other implementation details can be found in Appendix C.

In Stage 2, we use top- k percent approach to binarize scores and create the final filter, subsequently training a second CLIP model *on the curated dataset* to validate resulting filter’s effectiveness.

Expected Results. We anticipate mimic scores help large-scale training focus on high-value samples and can serve as instrumental metric for automating effective data curation.

Baselines. For the first stage, we compare Grad-Mimic to vanilla training, where each sample contributes in the weight update equally. For Stage 2 comparison, we compare our mimic score-based filter against the following methods: (1) *No Filtering*: using the entire training pool, (2) *Basic Filtering* [21]: selecting samples based on predefined criteria like caption length, image size, and caption language—representing a *human-designed filter*, (3) *CLIP Score* [22]: selecting top- k percent samples based on embedding alignments between images and captions. Scores are computed by OpenAI’s CLIP ViT-B/32 model pretrained on over 400 million samples [3]. We see CLIP score as a strong baseline, as it is prebuilt through heavy training using hundreds of millions of samples.

Stage 1 Results. Table 3 presents pretraining results for CLIP models on both dataset scales. Grad-Mimic consistently outperforms standard training at all temperature settings. Full results using various temperatures are provided in Appendix F. Interestingly, we find that mimicking the last layer of the image encoder yields more performance gains compared to targeting the text encoder. Figure 4 (left) presents the learning curves for CLIP

²We identified that some URLs provided by DataComp dataset are now broken. This means that our results might not be comparable to previous approaches on the DataComp Leaderboard. See [here](#) for details.

³<https://huggingface.co/laion/CLIP-ViT-B-32-DataComp.XL-s13B-b90K>

Scale	Filtering Strategy	Dataset Size	ImageNet	ImageNet dis. shifts	VTAB	Retrieval	Average over 38 datasets (\uparrow)
Small	No Filtering	10.7M	0.026	0.035	0.139	0.114	0.131
	Basic Filtering	3M	0.031	0.040	0.159	0.115	0.141
	Mimic Score Top 30%	3M	0.028	0.037	0.151	0.107	0.135
	Mimic Score Top 35%	3.8M	0.026	0.037	0.158	0.107	0.143
	Mimic Score Top 40%	4.2M	0.028	0.035	0.151	0.110	0.139
	CLIP Score (B/32 Top 30%)	3M	0.051	0.054	0.183	0.118	0.165
	CLIP Score \ Mimic Score Bottom 15%	2.7M (0.3M \downarrow)	0.047	0.053	0.174	0.106	0.163
Medium	CLIP Score \ Mimic Score Bottom 20%	2.6M (0.4M \downarrow)	0.047	0.052	0.173	0.113	0.164
	No Filtering	101.9M	0.026	0.035	0.139	0.114	0.254
	Basic Filtering	30M	0.209	0.176	0.264	0.232	0.267
	Mimic Score Top 30%	29M (1M \downarrow)	0.192	0.163	0.269	0.218	0.268
	CLIP Score (B/32 Top 30%)	30M	0.275	0.229	0.332	0.246	0.321
	CLIP Score \ Mimic Score Bottom 5%	28.1M (1.9M \downarrow)	0.270	0.227	0.339	0.246	0.323
	CLIP Score \ Mimic Score Bottom 10%	27.7M (2.3M \downarrow)	0.274	0.226	0.334	0.243	0.323
	CLIP Score \ Mimic Score Bottom 30%	25.3M (4.7M \downarrow)	0.264	0.223	0.330	0.244	0.322

Table 4: **Stage 2 Results in DataComp Experiment:** Mimic score-based filters perform better than basic filtering and complement CLIP score-based filters by removing low-value samples. Symbol “\” denotes the exclusion of curated datasets.

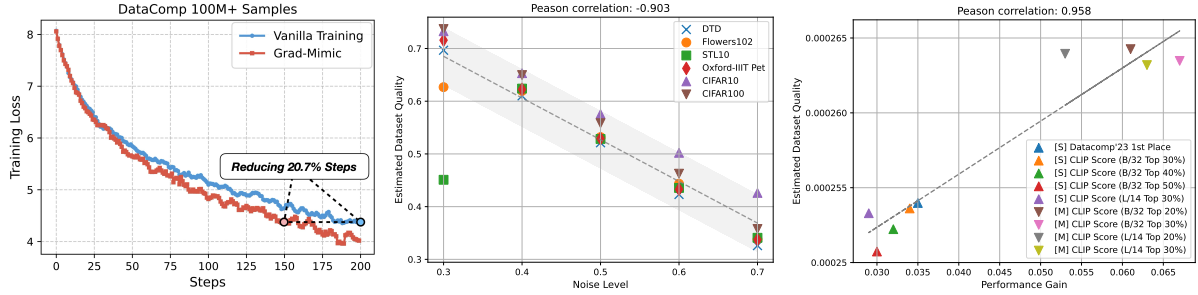


Figure 4: The left figure shows mimic score-guided training converges faster than vanilla baseline. The middle one uses retention rate to estimate training dataset quality in simulation experiments. The right figure takes the average on mimic scores in each curated dataset for performance gain estimation. [S/M] denotes the scale of DataComp dataset, small [S] or medium [M], that the filter is designed on.

models trained with Grad-Mimic versus the vanilla method. By re-weighting samples based on mimic scores in weight updates, Grad-Mimic achieves faster convergence, requiring **20.7%** fewer steps. These findings highlight Grad-Mimic’s success in *leveraging online pretrained weights to prioritize high-value samples for efficient training*.

Stage 2 Results. We use the derived mimic scores from our best-performing model in Stage 1 to design filters and evaluate their effectiveness. Results are presented in Table 4. Grad-Mimic automates the selection, outperforming basic filtering strategy at both scales. Additionally, we remove low-value samples ranked by mimic score to improve CLIP score-based filter (B/32 Top 30%). This complementary approach not only enhances model performance but also improves data efficiency by reducing training set size, *specifically removing 4.7 million samples in the medium-scale dataset*.

Lastly, we gather mimic scores from datasets that are curated by various CLIP score-based filters. We include the top-ranked approach during our time of experimentation [55], which uses an orthogonal approach based on object detection models. We average samples’ mimic scores in each curated dataset to estimate dataset quality and compare with their corresponding performance gains. The results, shown in Figure 4 (right), reveal a positive alignment with a Pearson correlation of **0.958**, demonstrating the feasibility to use mimic score as a reliable metric to predict potential model performance gains.

Sample Analysis. We analyze high- and low-value samples ranked by mimic score. In Figure 5, we compare token usage in captions. We find that bottom-ranked samples often carry captions that are either too short (1-2 words) or excessively long (over the maximum token limit), unlike top-ranked samples. Moreover, mimic score-based filter effectively identifies low-value samples, such as misaligned-caption images in the medium-scale dataset (see

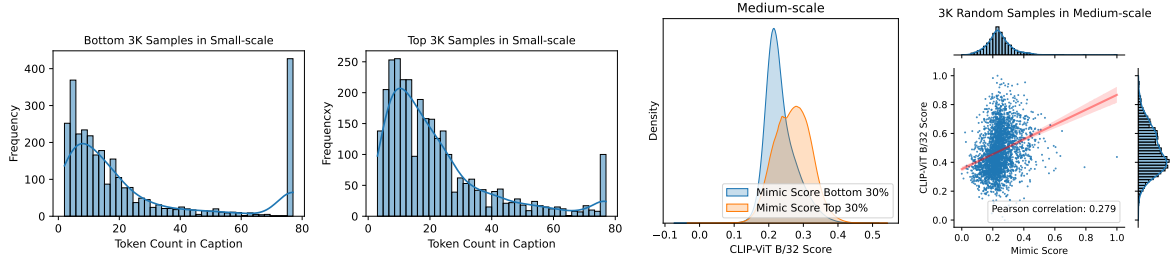


Figure 5: The left two figures compare token counts of bottom- and top-ranked samples by mimic score. The filtering logic matches handcrafted heuristics, particularly in caption length, where low-value samples have captions that are either *too short* or *over the 77-token limit*. The right two figures show mimic score distribution and its correlation with CLIP score.

Filtering Strategy	Random Selection		Mimic Score Selection	
	Jaccard Similarity	Percentage of Overlap	Jaccard Similarity	Percentage of Overlap
CLIP-ViT B/32 Top 30%	0.149	0.258	0.232	0.376
CLIP-ViT L/14 Top 30%	0.150	0.260	0.236	0.382
DataComp’23 Top-ranked [55]	0.166	0.284	0.271	0.426

Table 5: Mimic score can help in predicting whether a sample was used to train the reference model.

examples in Figure 1). *These filtering patterns align with human intuition but are automatically captured by Grad-Mimic.*

We visualize the top and bottom 30% of samples along with their CLIP scores in Figure 5. High-value samples align with higher CLIP scores, while low-value ones are more concentrated in the lower range (half below 0.2). Furthermore, we calculate their correlation on random samples. We normalize both scores into the range 0 to 1 for clarity. The observed positive correlation supports mimic scores in identifying high-quality samples (those have high CLIP score).

Predicting Pretraining Dataset. We explore an interesting application of mimic score: predicting the pretraining dataset. Specifically, we ask: *how accurately can Grad-Mimic check whether a given sample was used to train a reference model?* We test this hypothesis on the small-scale DataComp dataset. We first apply various pre-built filters to curate datasets and train CLIP models on each. Then, we target their final-layer weights to mimic and apply Grad-Mimic to train on the entire data pool. Our goal is to see whether the top-ranked samples (matched in size to the curated datasets) identified by mimic score appear in their training dataset.

We evaluate our approach against random selection using Jaccard similarity and percentage of overlap. As shown in Table 5, mimic score-based selection identifies more samples used to train the reference model compared to random sampling. We achieve a **42.6%** overlap with DataComp’23 best-performing filtered dataset [55] *by simply mimicking final-layer weights without direct access to their filtering steps.*

6 Conclusion

We introduce Mimic Score, an efficient data quality metric that assesses samples’ utility in model weight updates. By measuring the alignment of gradients with the vector toward pretrained reference weights, Mimic Score enables precise data assessment. Leveraging this scoring metric, we develop Grad-Mimic, a two-stage framework that automates high-quality data selection. Theoretically, we study how mimic score-guided training can converge faster than gradient descent. Empirically, Grad-Mimic effectively improves data efficiency, accelerating model convergence, and accurately detect mislabeled samples. The resulting filters outperform human-designed ones, and their statistics exhibit a strong correlation to training dataset quality and model performance improvements.

7 Acknowledgments

We thank Kwei-Herng Lai, Prasad Gabbur, Meng Cao, Ryan Jia, Russ Webb, Vedant Joshi, Albert Ge, Harit Vishwakarma, Dyah Adila, Changho Shin, Satya Sai Srinath Namburi, Zhiqi Gao, Avi Trost, and Gabe Orlanski for their helpful feedback and valuable discussion.

References

- [1] Fini, E.; Shukor, M.; Li, X.; Dufter, P.; Klein, M.; Haldimann, D.; Aitharaju, S.; da Costa, V. G. T.; Béthune, L.; Gan, Z.; others Multimodal autoregressive pre-training of large vision encoders. *arXiv preprint arXiv:2411.14402* **2024**,
- [2] Jia, C.; Yang, Y.; Xia, Y.; Chen, Y.-T.; Parekh, Z.; Pham, H.; Le, Q.; Sung, Y.-H.; Li, Z.; Duerig, T. Scaling up visual and vision-language representation learning with noisy text supervision. *International conference on machine learning*. 2021; pp 4904–4916.
- [3] Radford, A.; Kim, J. W.; Hallacy, C.; Ramesh, A.; Goh, G.; Agarwal, S.; Sastry, G.; Askell, A.; Mishkin, P.; Clark, J.; others Learning transferable visual models from natural language supervision. *International conference on machine learning*. 2021; pp 8748–8763.
- [4] Zhai, X.; Mustafa, B.; Kolesnikov, A.; Beyer, L. Sigmoid loss for language image pre-training. *Proceedings of the IEEE/CVF international conference on computer vision*. 2023; pp 11975–11986.
- [5] Albalak, A.; Elazar, Y.; Xie, S. M.; Longpre, S.; Lambert, N.; Wang, X.; Muennighoff, N.; Hou, B.; Pan, L.; Jeong, H.; others A survey on data selection for language models. *arXiv preprint arXiv:2402.16827* **2024**,
- [6] Bai, T.; Liang, H.; Wan, B.; Yang, L.; Li, B.; Wang, Y.; Cui, B.; He, C.; Yuan, B.; Zhang, W. A Survey of Multimodal Large Language Model from A Data-centric Perspective. *arXiv preprint arXiv:2405.16640* **2024**,
- [7] Penedo, G.; Kydliček, H.; Lozhkov, A.; Mitchell, M.; Raffel, C.; Von Werra, L.; Wolf, T.; others The fineweb datasets: Decanting the web for the finest text data at scale. *arXiv preprint arXiv:2406.17557* **2024**,
- [8] Wang, Y.; Chen, Y.; Yan, W.; Fang, A.; Zhou, W.; Jamieson, K.; Du, S. S. CLIPLoss and Norm-Based Data Selection Methods for Multimodal Contrastive Learning. *arXiv preprint arXiv:2405.19547* **2024**,
- [9] Thrush, T.; Potts, C.; Hashimoto, T. Improving pretraining data using perplexity correlations. *arXiv preprint arXiv:2409.05816* **2024**,
- [10] Fang, A.; Jose, A. M.; Jain, A.; Schmidt, L.; Toshev, A.; Shankar, V. Data filtering networks. *arXiv preprint arXiv:2309.17425* **2023**,
- [11] Chen, J.; Mueller, J. Automated data curation for robust language model fine-tuning. *arXiv preprint arXiv:2403.12776* **2024**,
- [12] Wettig, A.; Gupta, A.; Malik, S.; Chen, D. Qurating: Selecting high-quality data for training language models. *arXiv preprint arXiv:2402.09739* **2024**,
- [13] Thakkar, M.; Bolukbasi, T.; Ganapathy, S.; Vashishth, S.; Chandar, S.; Talukdar, P. Self-influence guided data reweighting for language model pre-training. *arXiv preprint arXiv:2311.00913* **2023**,
- [14] Mindermann, S.; Brauner, J. M.; Razzak, M. T.; Sharma, M.; Kirsch, A.; Xu, W.; Hölten, B.; Gomez, A. N.; Morisot, A.; Farquhar, S.; others Prioritized training on points that are learnable, worth learning, and not yet learnt. *International Conference on Machine Learning*. 2022; pp 15630–15649.
- [15] Lin, Z.; Gou, Z.; Gong, Y.; Liu, X.; Shen, Y.; Xu, R.; Lin, C.; Yang, Y.; Jiao, J.; Duan, N.; others Rho-1: Not all tokens are what you need. *arXiv preprint arXiv:2404.07965* **2024**,
- [16] Lin, X.; Wang, W.; Li, Y.; Yang, S.; Feng, F.; Wei, Y.; Chua, T.-S. Data-efficient Fine-tuning for LLM-based Recommendation. *Proceedings of the 47th International ACM SIGIR Conference on Research and Development in Information Retrieval*. 2024; pp 365–374.
- [17] Yu, Z.; Das, S.; Xiong, C. MATES: Model-Aware Data Selection for Efficient Pretraining with Data Influence Models. *arXiv preprint arXiv:2406.06046* **2024**,
- [18] Wang, J. T.; Wu, T.; Song, D.; Mittal, P.; Jia, R. GREATS: Online selection of high-quality data for llm training in every iteration. *Advances in Neural Information Processing Systems* **2024**, 37, 131197–131223.

- [19] Xia, M.; Malladi, S.; Gururangan, S.; Arora, S.; Chen, D. Less: Selecting influential data for targeted instruction tuning. *arXiv preprint arXiv:2402.04333* **2024**,
- [20] Wu, X.; Xia, M.; Shao, R.; Deng, Z.; Koh, P. W.; Russakovsky, O. ICONS: Influence Consensus for Vision-Language Data Selection. *arXiv preprint arXiv:2501.00654* **2024**,
- [21] Gadre, S. Y.; Ilharco, G.; Fang, A.; Hayase, J.; Smyrnis, G.; Nguyen, T.; Marten, R.; Wortsman, M.; Ghosh, D.; Zhang, J.; others Datacomp: In search of the next generation of multimodal datasets. *Advances in Neural Information Processing Systems* **2024**, 36.
- [22] Hessel, J.; Holtzman, A.; Forbes, M.; Bras, R. L.; Choi, Y. Clipscore: A reference-free evaluation metric for image captioning. *arXiv preprint arXiv:2104.08718* **2021**,
- [23] Fan, S.; Pagliardini, M.; Jaggi, M. Doge: Domain reweighting with generalization estimation. *arXiv preprint arXiv:2310.15393* **2023**,
- [24] Xie, S. M.; Pham, H.; Dong, X.; Du, N.; Liu, H.; Lu, Y.; Liang, P. S.; Le, Q. V.; Ma, T.; Yu, A. W. Doremi: Optimizing data mixtures speeds up language model pretraining. *Advances in Neural Information Processing Systems* **2024**, 36.
- [25] Chen, M. F.; Hu, M. Y.; Lourie, N.; Cho, K.; Ré, C. Aioli: A Unified Optimization Framework for Language Model Data Mixing. *arXiv preprint arXiv:2411.05735* **2024**,
- [26] Ge, A.; Huang, T.-H.; Cooper, J.; Trost, A.; Chu, Z.; GNVV, S. S. S. N.; Cai, Z.; Park, K.; Roberts, N.; Sala, F. R&B: Domain Regrouping and Data Mixture Balancing for Efficient Foundation Model Training. *arXiv preprint arXiv:2505.00358* **2025**,
- [27] Paul, S.; Raffel, C.; Schoenholz, S. S. Deep Learning on a Data Diet: Finding Important Examples Early in Training. *Advances in Neural Information Processing Systems (NeurIPS)*. 2021.
- [28] Sedova, A.; Zellinger, L.; Roth, B. Learning with noisy labels by adaptive gradient-based outlier removal. *Joint European Conference on Machine Learning and Knowledge Discovery in Databases*. 2023; pp 237–253.
- [29] Killamsetty, R.; Pervaje, A.; Mirzasoleiman, B. Grad-Match: Gradient Matching based Data Subset Selection for Efficient Deep Model Training. *Advances in Neural Information Processing Systems (NeurIPS)*. 2021.
- [30] Mirzasoleiman, B.; Bilmes, J.; Leskovec, J. Coresets for data-efficient training of machine learning models. *International Conference on Machine Learning*. 2020; pp 6950–6960.
- [31] Schuhmann, C.; Beaumont, R.; Vencu, R.; Gordon, C.; Wightman, R.; Cherti, M.; Coombes, T.; Katta, A.; Mullis, C.; Wortsman, M.; others Laion-5b: An open large-scale dataset for training next generation image-text models. *Advances in Neural Information Processing Systems* **2022**, 35, 25278–25294.
- [32] Thomee, B.; Shamma, D. A.; Friedland, G.; Elizalde, B.; Ni, K.; Poland, D.; Borth, D.; Li, L.-J. Yfcc100m: The new data in multimedia research. *Communications of the ACM* **2016**, 59, 64–73.
- [33] Abbas, A.; Tirumala, K.; Simig, D.; Ganguli, S.; Morcos, A. S. Semdedup: Data-efficient learning at web-scale through semantic deduplication. *arXiv preprint arXiv:2303.09540* **2023**,
- [34] Ratner, A. J.; De Sa, C. M.; Wu, S.; Selsam, D.; Ré, C. Data programming: Creating large training sets, quickly. *Advances in neural information processing systems* **2016**, 29.
- [35] Ratner, A.; Bach, S. H.; Ehrenberg, H.; Fries, J.; Wu, S.; Ré, C. Snorkel: Rapid training data creation with weak supervision. *Proceedings of the VLDB Endowment. International Conference on Very Large Data Bases*. 2017; p 269.
- [36] Ratner, A.; Hancock, B.; Dunnmon, J.; Sala, F.; Pandey, S.; Ré, C. Training complex models with multi-task weak supervision. *Proceedings of the AAAI Conference on Artificial Intelligence*. 2019; pp 4763–4771.
- [37] Fu, D.; Chen, M.; Sala, F.; Hooper, S.; Fatahalian, K.; Ré, C. Fast and three-rious: Speeding up weak supervision with triplet methods. *International Conference on Machine Learning*. 2020; pp 3280–3291.
- [38] Huang, T.-H.; Cao, C.; Bhargava, V.; Sala, F. The ALChEmist: Automated Labeling 500x CHEaper Than LLM Data Annotators. *arXiv preprint arXiv:2407.11004* **2024**,
- [39] Huang, T.-H.; Cao, C.; Schoenberg, S.; Vishwakarma, H.; Roberts, N.; Sala, F. ScriptoriumWS: A Code Generation Assistant For Weak Supervision. *ICLR Deep Learning for Code Workshop* **2023**,

- [40] Hooper, S.; Wornow, M.; Seah, Y. H.; Kellman, P.; Xue, H.; Sala, F.; Langlotz, C.; Re, C. Cut out the annotator, keep the cutout: better segmentation with weak supervision. *International Conference on Learning Representations*. 2020.
- [41] Fries, J. A.; Varma, P.; Chen, V. S.; Xiao, K.; Tejeda, H.; Saha, P.; Dunnmon, J.; Chubb, H.; Maskatia, S.; Fiterau, M.; others Weakly supervised classification of aortic valve malformations using unlabeled cardiac MRI sequences. *Nature communications* **2019**, *10*, 3111.
- [42] Khattar, S.; O'Day, H.; Varma, P.; Fries, J.; Hicks, J.; Delp, S.; Bronte-Stewart, H.; Re, C. Multi-frame weak supervision to label wearable sensor data. *ICML Time Series Workshop*. 2019.
- [43] Roberts, N.; Li, X.; Huang, T.-H.; Adila, D.; Schoenberg, S.; Liu, C.-Y.; Pick, L.; Ma, H.; Albarghouthi, A.; Sala, F. Autows-bench-101: Benchmarking automated weak supervision with 100 labels. *Advances in Neural Information Processing Systems* **2022**, *35*, 8912–8925.
- [44] Shin, C.; Li, W.; Vishwakarma, H.; Roberts, N.; Sala, F. Universalizing weak supervision. *arXiv preprint arXiv:2112.03865* **2021**,
- [45] Ghiasi, A.; Kazemi, H.; Borgnia, E.; Reich, S.; Shu, M.; Goldblum, M.; Wilson, A. G.; Goldstein, T. What do vision transformers learn? a visual exploration. *arXiv preprint arXiv:2212.06727* **2022**,
- [46] Gandelsman, Y.; Efros, A. A.; Steinhart, J. Interpreting CLIP's Image Representation via Text-Based Decomposition. *arXiv preprint arXiv:2310.05916* **2023**,
- [47] Wu, X. Optimal quantization by matrix searching. *Journal of algorithms* **1991**, *12*, 663–673.
- [48] Cimpoi, M.; Maji, S.; Kokkinos, I.; Mohamed, S.; Vedaldi, A. Describing Textures in the Wild. *Proceedings of the IEEE Conference on Computer Vision and Pattern Recognition (CVPR)*. 2014; pp 3606–3613.
- [49] Nilsback, M.-E.; Zisserman, A. Automated flower classification over a large number of classes. *Proceedings of the Indian Conference on Computer Vision, Graphics and Image Processing* **2008**, 722–729.
- [50] Coates, A.; Ng, A. Y.; Lee, H. An Analysis of Single-Layer Networks in Unsupervised Feature Learning. *Proceedings of the International Conference on Artificial Intelligence and Statistics (AISTATS)*. 2011; pp 215–223.
- [51] Parkhi, O. M.; Vedaldi, A.; Zisserman, A.; Jawahar, C. Cats and Dogs. *Proceedings of the IEEE Conference on Computer Vision and Pattern Recognition (CVPR)*. 2012; pp 3498–3505.
- [52] Krizhevsky, A.; Hinton, G. *Learning Multiple Layers of Features from Tiny Images*; 2009.
- [53] Dosovitskiy, A. An image is worth 16x16 words: Transformers for image recognition at scale. *arXiv preprint arXiv:2010.11929* **2020**,
- [54] Cherti, M.; Beaumont, R.; Wightman, R.; Wortsman, M.; Ilharco, G.; Gordon, C.; Schuhmann, C.; Schmidt, L.; Jitsev, J. Reproducible scaling laws for contrastive language-image learning. *Proceedings of the IEEE/CVF Conference on Computer Vision and Pattern Recognition*. 2023; pp 2818–2829.
- [55] Huang, T.-H.; Shin, C.; Tay, S. J.; Adila, D.; Sala, F. Multimodal Data Curation via Object Detection and Filter Ensembles. *arXiv preprint arXiv:2401.12225* **2024**,
- [56] Russakovsky, O.; Deng, J.; Su, H.; Krause, J.; Satheesh, S.; Ma, S.; Huang, Z.; Karpathy, A.; Khosla, A.; Bernstein, M.; others Imagenet large scale visual recognition challenge. *International journal of computer vision* **2015**, *115*, 211–252.
- [57] Hampel, F. R. The influence curve and its role in robust estimation. *Journal of the american statistical association* **1974**, *69*, 383–393.
- [58] Cook, R. D.; Weisberg, S. Characterizations of an empirical influence function for detecting influential cases in regression. *Technometrics* **1980**, *22*, 495–508.
- [59] Koh, P. W.; Liang, P. Understanding black-box predictions via influence functions. *International conference on machine learning*. 2017; pp 1885–1894.

Appendix Roadmap. Our appendix is structured as follows. It starts with a theoretical analysis of effective batch reweighting in Appendix A, studying conditions where Grad-Mimic’s online reweighting method outperforms standard gradient descent. Next, Appendix B outlines Grad-Mimic algorithms for both stages. This leads into detailed experimental setups, including training configurations and computational resources, presented in Appendix C. Then, we continue with Appendix D, comparing Grad-Mimic to other model-based data selection approaches. Following this, Appendix E provides a comprehensive analysis about Grad-Mimic’s efficiency advantages, substantiated by various evidence, compared to other baseline methods. Appendix F wraps up with ablation studies, examining temperature controls, choices of layer weights to mimic, and the impact of reference model quality. Finally, Appendix G concludes by discussing the broader impacts and limitations of this work.

A Theoretical Analysis

We first present a glossary table listing the defined notations and their meanings used in the following analysis.

Symbol	Meaning
\mathbb{E}	Expectation over inherent randomness, such as over gradient noise δ .
$\mathbb{E}^{(x)}$	Expectation over the dataset
$\sigma(\cdot)$	The softmax function
n	Dataset size
L	Smoothness parameter on loss function ℓ
δ	Level of the gradient noise, $\delta = \mathbb{E}[\ \delta_{i,t}\ ^2]$
ϵ	Parameter distance between reference model and the optimal model, $\epsilon = \ \theta_{\text{ref}} - \theta_*\ $
τ	Temperature parameter used in Grad-Mimic updates
v_t	Target vector induced by reference model, $\theta_{\text{ref}} - \theta_t$
$-a_{i,t}$	The alignment of the gradient of the loss with the target vector, $g_{i,t}^\top v_t$
λ_t	The softmax parameter, $1/(\tau\ v_t\)$
$\ell(\theta_t; s_i)$	The loss of the model with parameters θ_t on a given sample s_i
$g_{i,t}$	$\nabla\ell(\theta_t; s_i)$
$\tilde{g}_{i,t}$	$\nabla\ell(\theta_t; s_i) + \delta_{i,t}$ where $\delta_{i,t}$ is a noise term
θ_{t+1}^{gd}	The learned parameter through a standard GD update
θ_{t+1}^{gm}	The learned parameter through a Grad-Mimic update

We aim to analyze the convergence rates of standard Gradient Descent (GD) and the Grad-Mimic (GM) online reweighting algorithm for an L -smooth loss function ℓ , using noisy gradients with noise level δ . Our goal is to compare their convergence to the global minimum θ_* , explicitly incorporating the term $\epsilon = \|\theta_{\text{ref}} - \theta_*\|$ for Grad-Mimic. We start by specifying the update rules for both algorithms, then present three lemmas concerning adaptive algorithms and the softmax function. Finally, we discuss how these results apply to Grad-Mimic and quantify the improvement over GD.

Problem Setup. Consider a (potentially noisy) dataset $D = \{s_i\}_{i=1}^n$ and an L -smooth loss function $\ell(\theta; s)$, defined as:

$$\ell(\theta) = \frac{1}{n} \sum_{i=1}^n \ell(\theta; s_i).$$

The function ℓ is L -smooth, and its global minimum is denoted by θ_* . We assume access to noisy gradients:

$$\tilde{g}_{i,t} = g_{i,t} + \delta_{i,t},$$

where the gradient noise $\delta_{i,t}$ satisfies:

$$\mathbb{E}[\delta_{i,t}] = 0, \quad \mathbb{E}[\|\delta_{i,t}\|^2] = \delta.$$

Additionally, we have a reference solution θ_{ref} closer to the optimum than the initial weight θ_0 in the weight space:

$$\|\theta_0 - \theta_*\| \gg \|\theta_{\text{ref}} - \theta_*\| = \epsilon.$$

Standard Gradient Descent. An update rule for GD at iteration t is:

$$\theta_{t+1}^{\text{gd}} = \theta_t - \eta \frac{1}{n} \sum_{i=1}^n \tilde{g}_{i,t}. \quad (4)$$

Grad-Mimic's Online Reweighting. An update rule for Grad-Mimic at iteration t is:

$$\theta_{t+1}^{\text{gm}} = \theta_t - \frac{\eta}{\sum_{i=1}^n \alpha_{i,t}} \sum_{i=1}^n \alpha_{i,t} \tilde{g}_{i,t}, \quad (5)$$

with adaptive weighting that:

$$\begin{aligned} v_t &= \theta_{\text{ref}} - \theta_t, \\ m_{i,t} &= -\tilde{g}_{i,t}^\top v_t / \|v_t\|, \\ \alpha_{i,t} &= e^{m_{i,t}/\tau}. \end{aligned}$$

This adaptive weighting leverages the proximity of the reference point θ_{ref} to the true minimum θ_* , which is expected to effectively mitigating gradient noise. When it is convenient, the following notation is used:

$$\begin{aligned} a_{i,t} &= -\tilde{g}_{i,t}^\top v_t, \\ \lambda &= 1/(\tau \|v_t\|), \end{aligned}$$

so that

$$\alpha_{i,t} = \exp(\lambda a_{i,t}).$$

We begin with a lemma about *any adaptive weighting procedure*, where the $\alpha_{i,t}$ (written as α_i unless the timestep needs to be specified) terms are unconstrained.

Lemma A.1. *Let*

$$R = 2\text{Cov}^{(x)}\left(\frac{\alpha_i}{\mathbb{E}^{(x)}[\alpha_i]}, a_{i,t}\right) - \eta(\|\mathbb{E}^{(x)}[\frac{\alpha_i}{\mathbb{E}^{(x)}[\alpha_i]} \tilde{g}_{i,t}]\|^2 - \|\mathbb{E}^{(x)}[\tilde{g}_{i,t}]\|^2)$$

Then

$$\|\theta_{t+1}^{\text{gm}} - \theta_{\text{ref}}\|^2 = \|\theta_{t+1}^{\text{gd}} - \theta_{\text{ref}}\|^2 - \eta R$$

Proof. First, begin with a calculation of what $\|\theta_{t+1}^{\text{gm}} - \theta_{\text{ref}}\|^2$ is.

$$\begin{aligned} \|\theta_{t+1}^{\text{gm}} - \theta_{\text{ref}}\|^2 &= \|\theta_t - \eta \frac{\sum_{i=1}^n \alpha_i \tilde{g}_{i,t}}{\sum_{i=1}^n \alpha_i} - \theta_{\text{ref}}\|^2 \\ &= \|\theta_t - \eta \frac{\mathbb{E}^{(x)}[\alpha_i \tilde{g}_{i,t}]}{\mathbb{E}^{(x)}[\alpha_i]} - \theta_{\text{ref}}\|^2 \\ &= \|\theta_t - \theta_{\text{ref}}\|^2 - 2\eta(\theta_t - \theta_{\text{ref}})^\top \frac{\mathbb{E}^{(x)}[\alpha_i \tilde{g}_{i,t}]}{\mathbb{E}^{(x)}[\alpha_i]} + \eta^2 \left\| \frac{\mathbb{E}^{(x)}[\alpha_i \tilde{g}_{i,t}]}{\mathbb{E}^{(x)}[\alpha_i]} \right\|^2 \\ &= \|\theta_t - \theta_{\text{ref}}\|^2 + 2\eta \frac{\mathbb{E}^{(x)}[\alpha_i v_t^\top \tilde{g}_{i,t}]}{\mathbb{E}^{(x)}[\alpha_i]} + \eta^2 \frac{\|\mathbb{E}^{(x)}[\alpha_i \tilde{g}_{i,t}]\|^2}{\mathbb{E}^{(x)}[\alpha_i]^2} \end{aligned}$$

Next, using the following identities,

$$\begin{aligned} \frac{\mathbb{E}^{(x)}[\alpha_i v_t^\top \tilde{g}_{i,t}]}{\mathbb{E}^{(x)}[\alpha_i]} &= \frac{\mathbb{E}^{(x)}[\alpha_i v_t^\top \tilde{g}_{i,t}] - \mathbb{E}^{(x)}[\alpha_i] \mathbb{E}^{(x)}[v_t^\top \tilde{g}_{i,t}] + \mathbb{E}^{(x)}[\alpha_i] \mathbb{E}^{(x)}[v_t^\top \tilde{g}_{i,t}]}{\mathbb{E}^{(x)}[\alpha_i]} \\ &= \mathbb{E}^{(x)}[v_t^\top \tilde{g}_{i,t}] + \frac{\mathbb{E}^{(x)}[\alpha_i v_t^\top \tilde{g}_{i,t}] - \mathbb{E}^{(x)}[\alpha_i] \mathbb{E}^{(x)}[v_t^\top \tilde{g}_{i,t}]}{\mathbb{E}^{(x)}[\alpha_i]} \\ &= \mathbb{E}^{(x)}[v_t^\top \tilde{g}_{i,t}] + \frac{\text{Cov}^{(x)}(\alpha_i, v_t^\top \tilde{g}_{i,t})}{\mathbb{E}^{(x)}[\alpha_i]} \end{aligned}$$

and

$$\begin{aligned}
\frac{\|\mathbb{E}^{(x)}[\alpha_i \tilde{g}_{i,t}]\|^2}{\mathbb{E}^{(x)}[\alpha_i]^2} &= \frac{\|\mathbb{E}^{(x)}[\alpha_i \tilde{g}_{i,t}]\|^2 - \mathbb{E}^{(x)}[\alpha_i]^2 \|\mathbb{E}^{(x)}[\tilde{g}_{i,t}]\|^2 + \mathbb{E}^{(x)}[\alpha_i]^2 \|\mathbb{E}^{(x)}[\tilde{g}_{i,t}]\|^2}{\mathbb{E}^{(x)}[\alpha_i]^2} \\
&= \|\mathbb{E}^{(x)}[\tilde{g}_{i,t}]\|^2 + \frac{\|\mathbb{E}^{(x)}[\alpha_i \tilde{g}_{i,t}]\|^2 - \mathbb{E}^{(x)}[\alpha_i]^2 \|\mathbb{E}^{(x)}[\tilde{g}_{i,t}]\|^2}{\mathbb{E}^{(x)}[\alpha_i]^2} \\
&= \|\mathbb{E}^{(x)}[\tilde{g}_{i,t}]\|^2 + \frac{\|\mathbb{E}^{(x)}[\alpha_i \tilde{g}_{i,t}]\|^2 - \|\mathbb{E}^{(x)}[\alpha_i] \mathbb{E}^{(x)}[\tilde{g}_{i,t}]\|^2}{\mathbb{E}^{(x)}[\alpha_i]^2}
\end{aligned}$$

We can proceed as

$$\begin{aligned}
\|\theta_{t+1}^{\text{gm}} - \theta_{\text{ref}}\|^2 &= \|\theta_t - \theta_{\text{ref}}\|^2 + 2\eta \left(\mathbb{E}^{(x)}[v_t^\top \tilde{g}_{i,t}] + \frac{\text{Cov}^{(x)}(\alpha_i, v_t^\top \tilde{g}_{i,t})}{\mathbb{E}^{(x)}[\alpha_i]} \right) \\
&\quad + \eta^2 \left(\|\mathbb{E}^{(x)}[\tilde{g}_{i,t}]\|^2 + \frac{\|\mathbb{E}^{(x)}[\alpha_i \tilde{g}_{i,t}]\|^2 - \|\mathbb{E}^{(x)}[\alpha_i] \mathbb{E}^{(x)}[\tilde{g}_{i,t}]\|^2}{\mathbb{E}^{(x)}[\alpha_i]^2} \right) \\
&= \|\theta_t - \theta_{\text{ref}}\|^2 + 2\eta \mathbb{E}^{(x)}[v_t^\top \tilde{g}_{i,t}] + \eta^2 \|\mathbb{E}^{(x)}[\tilde{g}_{i,t}]\|^2 \\
&\quad + 2\eta \frac{\text{Cov}^{(x)}(\alpha_i, v_t^\top \tilde{g}_{i,t})}{\mathbb{E}^{(x)}[\alpha_i]} + \eta^2 \frac{\|\mathbb{E}^{(x)}[\alpha_i \tilde{g}_{i,t}]\|^2 - \|\mathbb{E}^{(x)}[\alpha_i] \mathbb{E}^{(x)}[\tilde{g}_{i,t}]\|^2}{\mathbb{E}^{(x)}[\alpha_i]^2} \\
&= \|\theta_{t+1}^{\text{gd}} - \theta_{\text{ref}}\|^2 + 2\eta \frac{\text{Cov}^{(x)}(\alpha_i, v_t^\top \tilde{g}_{i,t})}{\mathbb{E}^{(x)}[\alpha_i]} + \eta^2 \frac{\|\mathbb{E}^{(x)}[\alpha_i \tilde{g}_{i,t}]\|^2 - \|\mathbb{E}^{(x)}[\alpha_i] \mathbb{E}^{(x)}[\tilde{g}_{i,t}]\|^2}{\mathbb{E}^{(x)}[\alpha_i]^2} \\
&= \|\theta_{t+1}^{\text{gd}} - \theta_{\text{ref}}\|^2 + 2\eta \text{Cov}^{(x)}\left(\frac{\alpha_i}{\mathbb{E}^{(x)}[\alpha_i]}, v_t^\top \tilde{g}_{i,t}\right) + \eta^2 (\|\mathbb{E}^{(x)}[\frac{\alpha_i}{\mathbb{E}^{(x)}[\alpha_i]} \tilde{g}_{i,t}]\|^2 - \|\mathbb{E}^{(x)}[\tilde{g}_{i,t}]\|^2) \\
&= \|\theta_{t+1}^{\text{gd}} - \theta_{\text{ref}}\|^2 - 2\eta \text{Cov}^{(x)}\left(\frac{\alpha_i}{\mathbb{E}^{(x)}[\alpha_i]}, a_{i,t}\right) + \eta^2 (\|\mathbb{E}^{(x)}[\frac{\alpha_i}{\mathbb{E}^{(x)}[\alpha_i]} \tilde{g}_{i,t}]\|^2 - \|\mathbb{E}^{(x)}[\tilde{g}_{i,t}]\|^2) \\
&= \|\theta_{t+1}^{\text{gd}} - \theta_{\text{ref}}\|^2 - \eta R
\end{aligned}$$

□

From Lemma A.1, we want to bound R to hopefully show that $R > 0$, indicating that taking an update step with Grad-Mimic will converge faster than GD.

Lemma A.2. Let $f(\lambda) = \frac{\sum_{i=1}^n \exp(\lambda v_i) v_i}{\sum_{i=1}^n \exp(\lambda v_i)}$ and $\sigma(\lambda)$ be the vector where $\sigma(\lambda)_i = \frac{\exp(\lambda v_i)}{\sum_{j=1}^n \exp(\lambda v_j)}$. Then

$$f(\lambda) - f(0) \geq \frac{1}{\lambda} \|\sigma(\lambda) - \sigma(0)\|^2$$

Proof. Following the definitions,

$$\begin{aligned}
f(\lambda) - f(0) &= \sigma(\lambda)^\top v - \sigma(0)^\top v \\
&= (\sigma(\lambda) - \sigma(0))^\top (v - 0)
\end{aligned}$$

Now, fix a λ . Abusing notation, let $\sigma(v)_i = \frac{\exp(\lambda v_i)}{\sum_{j=1}^n \exp(\lambda v_j)}$, where λ is now fixed and the vector v is variable. As such, $f(\lambda) - f(0) = (\sigma(v) - \sigma(0))^\top (v - 0)$. Since $\sigma(\cdot)$ is λ -Lipschitz, it follows that

$$(\sigma(v) - \sigma(0))^\top (v - 0) \geq \frac{1}{\lambda} \|\sigma(v) - \sigma(0)\|^2$$

then we can have

$$f(\lambda) - f(0) \geq \frac{1}{\lambda} \|\sigma(\lambda) - \sigma(0)\|^2$$

□

Lemma A.3. The value of R in Grad-Mimic is guaranteed to be positive if

$$\eta < \frac{2\tau \|v_t\| \cdot \|\sigma(1/\tau \|v_t\|) - \sigma(0)\|^2}{\|\mathbb{E}^{(x)}[\frac{\alpha_i}{\mathbb{E}^{(x)}[\alpha_i]} \tilde{g}(\theta_t; s_i)]\|^2 - \|\mathbb{E}^{(x)}[\tilde{g}(\theta_t; s_i)]\|^2},$$

or $\|\mathbb{E}^{(x)}[\frac{\alpha_i}{\mathbb{E}^{(x)}[\alpha_i]} \tilde{g}(\theta_t; s_i)]\|^2 \leq \|\mathbb{E}^{(x)}[\tilde{g}(\theta_t; s_i)]\|^2$.

Proof. First, recall

$$R = 2\text{Cov}^{(x)}\left(\frac{\alpha_i}{\mathbb{E}^{(x)}[\alpha_i]}, (\theta_t - \theta_{\text{ref}})^\top \tilde{g}(\theta_t; s_i)\right) - \eta(\|\mathbb{E}^{(x)}[\frac{\alpha_i}{\mathbb{E}^{(x)}[\alpha_i]} \tilde{g}(\theta_t; s_i)]\|^2 - \|\mathbb{E}^{(x)}[\tilde{g}(\theta_t; s_i)]\|^2)$$

Inspecting the first term, as a result of the previous lemma,

$$\begin{aligned} \text{Cov}^{(x)}\left(\frac{\alpha_i}{\mathbb{E}^{(x)}[\alpha_i]}, (\theta_t - \theta_{\text{ref}})^\top \tilde{g}(\theta_t; s_i)\right) &= \text{Cov}^{(x)}\left(\frac{\alpha_i}{\mathbb{E}^{(x)}[\alpha_i]}, \tilde{a}_{i,t}\right) \\ &= \mathbb{E}^{(x)}\left[\frac{\alpha_i}{\mathbb{E}^{(x)}[\alpha_i]} \tilde{a}_{i,t}\right] - \mathbb{E}^{(x)}[\tilde{a}_{i,t}] \\ &= \frac{\sum_{i=1}^n \alpha_i \tilde{a}_{i,t}}{\sum_{i=1}^n \alpha_i} - \frac{\sum_{i=1}^n \exp(0) \tilde{a}_{i,t}}{\sum_{i=1}^n \exp(0)} \\ &= \frac{\sum_{i=1}^n \exp(\lambda \tilde{a}_{i,t}) \tilde{a}_{i,t}}{\sum_{i=1}^n \exp(\lambda \tilde{a}_{i,t})} - \frac{\sum_{i=1}^n \exp(0 \tilde{a}_{i,t}) \tilde{a}_{i,t}}{\sum_{i=1}^n \exp(0 \tilde{a}_{i,t})} \\ &= f(\lambda) - f(0) \\ &\geq \frac{1}{\lambda} \|\sigma(\lambda) - \sigma(0)\|^2 \end{aligned}$$

Thus,

$$R \geq \frac{2}{\lambda} \|\sigma(\lambda) - \sigma(0)\|^2 - \eta(\|\mathbb{E}^{(x)}[\frac{\alpha_i}{\mathbb{E}^{(x)}[\alpha_i]} \tilde{g}(\theta_t; s_i)]\|^2 - \|\mathbb{E}^{(x)}[\tilde{g}(\theta_t; s_i)]\|^2)$$

Finally, with the definition $\lambda = 1/(\tau\|v_t\|)$,

$$R \geq 2\tau\|v_t\| \cdot \|\sigma(1/\tau\|v_t\|) - \sigma(0)\|^2 - \eta(\|\mathbb{E}^{(x)}[\frac{\alpha_i}{\mathbb{E}^{(x)}[\alpha_i]} \tilde{g}(\theta_t; s_i)]\|^2 - \|\mathbb{E}^{(x)}[\tilde{g}(\theta_t; s_i)]\|^2)$$

A sufficient condition for $R > 0$ is therefore given by

$$\eta < \frac{2\tau\|v_t\| \cdot \|\sigma(1/\tau\|v_t\|) - \sigma(0)\|^2}{\|\mathbb{E}^{(x)}[\frac{\alpha_i}{\mathbb{E}^{(x)}[\alpha_i]} \tilde{g}(\theta_t; s_i)]\|^2 - \|\mathbb{E}^{(x)}[\tilde{g}(\theta_t; s_i)]\|^2}$$

□

So far, the only quantity being bounded is the distance to the reference model θ_{ref} . Lastly, we extend to bound convergence to the optimum θ_* and present our Theorem A.4 by using 3 lemma above.

Theorem A.4. *Let $\kappa = \max_i \|\tilde{g}(\theta_t; s_i)\|$. Then*

$$\|\theta_{t+1}^{\text{gm}} - \theta_*\|^2 \leq \|\theta_{t+1}^{\text{gd}} - \theta_*\|^2 - \eta[2\tau\|v_t\| \cdot \|\sigma(1/\tau\|v_t\|) - \sigma(0)\|^2 - 4\epsilon\kappa - \eta\kappa^2]$$

Specifically, if $\eta < \frac{2\tau\|v_t\| \cdot \|\sigma(1/\tau\|v_t\|) - \sigma(0)\|^2 - 4\epsilon\kappa}{\kappa^2}$ then $\|\theta_{t+1}^{\text{gm}} - \theta_\| \leq \|\theta_{t+1}^{\text{gd}} - \theta_*\|$.*

Proof. Starting with an application of Lemma A.1,

$$\begin{aligned} \|\theta_{t+1}^{\text{gm}} - \theta_*\|^2 &= \|\theta_{t+1}^{\text{gm}} - \theta_{\text{ref}}\|^2 + \|\theta_{\text{ref}} - \theta_*\|^2 + 2(\theta_{t+1}^{\text{gm}} - \theta_{\text{ref}})^\top (\theta_{\text{ref}} - \theta_*) \\ &= \|\theta_{t+1}^{\text{gd}} - \theta_{\text{ref}}\|^2 + \|\theta_{\text{ref}} - \theta_*\|^2 + 2(\theta_{t+1}^{\text{gm}} - \theta_{\text{ref}})^\top (\theta_{\text{ref}} - \theta_*) - \eta R \\ &= \|\theta_{t+1}^{\text{gd}} - \theta_*\|^2 - 2(\theta_{t+1}^{\text{gd}} - \theta_{\text{ref}})^\top (\theta_{\text{ref}} - \theta_*) + 2(\theta_{t+1}^{\text{gm}} - \theta_{\text{ref}})^\top (\theta_{\text{ref}} - \theta_*) - \eta R \\ &= \|\theta_{t+1}^{\text{gd}} - \theta_*\|^2 + 2(\theta_{t+1}^{\text{gm}} - \theta_{t+1}^{\text{gd}})^\top (\theta_{\text{ref}} - \theta_*) - \eta R \\ &\leq \|\theta_{t+1}^{\text{gd}} - \theta_*\|^2 + 2\epsilon\|\theta_{t+1}^{\text{gd}} - \theta_{t+1}^{\text{gm}}\| - \eta R \end{aligned}$$

Thus, we achieve superior performance towards the optimum if

$$R > \frac{2\epsilon\|\theta_{t+1}^{\text{gm}} - \theta_{t+1}^{\text{gd}}\|}{\eta}$$

Using Lemma A.3,

$$\begin{aligned}
\|\theta_{t+1}^{\text{gm}} - \theta_*\|^2 &\leq \|\theta_{t+1}^{\text{gd}} - \theta_*\|^2 + 2\epsilon\|\theta_{t+1}^{\text{gd}} - \theta_{t+1}^{\text{gm}}\| - \eta R \\
&\leq \|\theta_{t+1}^{\text{gd}} - \theta_*\|^2 + 2\epsilon\|\theta_{t+1}^{\text{gd}} - \theta_{t+1}^{\text{gm}}\| - 2\eta\tau\|v_t\| \cdot \|\sigma(1/\tau\|v_t\|) - \sigma(0)\|^2 \\
&\quad + \eta^2(\|\mathbb{E}^{(x)}[\frac{\alpha_i}{\mathbb{E}^{(x)}[\alpha_i]}\tilde{g}(\theta_t; s_i)]\|^2 - \|\mathbb{E}^{(x)}[\tilde{g}(\theta_t; s_i)]\|^2) \\
&\leq \|\theta_{t+1}^{\text{gd}} - \theta_*\|^2 + 4\epsilon\eta\kappa - 2\eta\tau\|v_t\| \cdot \|\sigma(1/\tau\|v_t\|) - \sigma(0)\|^2 \\
&\quad + \eta^2(\|\mathbb{E}^{(x)}[\frac{\alpha_i}{\mathbb{E}^{(x)}[\alpha_i]}\tilde{g}(\theta_t; s_i)]\|^2 - \|\mathbb{E}^{(x)}[\tilde{g}(\theta_t; s_i)]\|^2) \\
&\leq \|\theta_{t+1}^{\text{gd}} - \theta_*\|^2 + 4\epsilon\eta\kappa - 2\eta\tau\|v_t\| \cdot \|\sigma(1/\tau\|v_t\|) - \sigma(0)\|^2 + \eta^2\kappa^2
\end{aligned}$$

where the penultimate inequality uses $\|\theta_{t+1}^{\text{gm}} - \theta_{t+1}^{\text{gd}}\| \leq \|\theta_{t+1}^{\text{gm}}\| + \|\theta_{t+1}^{\text{gd}}\| \leq 2\eta\kappa$.

We then can find a bound of η for $\|\theta_{t+1}^{\text{gm}} - \theta_*\|^2 \leq \|\theta_{t+1}^{\text{gd}} - \theta_*\|^2$:

$$\eta < \frac{2\tau\|v_t\| \cdot \|\sigma(1/\tau\|v_t\|) - \sigma(0)\|^2 - 4\epsilon\kappa}{\kappa^2}.$$

□

Theorem A.4 Discussion. Our convergence bound reveals conditions under which Grad-Mimic outperforms GD. First, the learning rate η should be small. A large η causes the κ^2 term to dominate, leading to large, erroneous steps in Grad-Mimic compared to GD. This is particularly evident when the temperature is small, as Grad-Mimic amplifies specific gradients while GD averages conflicting ones, potentially overshooting the optimum if the gradient magnitude κ is large. Second, κ should be small to avoid similar overshooting issues. Third, $\epsilon = \|\theta_{\text{ref}} - \theta_*\|$ should be small. This follows from our intuition: a pre-trained reference model θ_{ref} serves as a proxy to the optimum θ_* , prioritizing weight movements toward this proxy can accelerate convergence.

B Grad-Mimic Algorithms

Here, we summarize algorithm steps. Grad-Mimic proceeds in two stages. Stage 1 (Sec. 4.1) computes mimic scores on the fly and updates model weights through re-weighting. Stage 2 (Sec. 4.2) binarizes mimic scores and aggregates utility assessments to obtain the final estimate. Our algorithm supports various training paradigms, including supervised learning and self-supervised learning, as demonstrated in Sec. 5.1 and Sec. 5.2. Our experiments encompass a range of training configurations, including *full-parameter fine-tuning*, *linear probing*, and *training models from scratch*.

Algorithm 1 Online Batch Reweighting (Stage 1)

Input: Reference model θ_{ref} , model being trained θ , dataset D , number of training steps T , batch size b , learning rate η , temperature parameter τ

Output: Normalized mimic scores $\bar{m}_{i,t}$ for each sample i at step t

- 1: Initialize model weights θ_0
 - 2: **for** $t = 1$ to T **do**
 - 3: Sample a batch $\{s_i\}_{i=1}^b$ uniformly from D
 - 4: $v_t \leftarrow \theta_{\text{ref}} - \theta_t$ ▷ Weight difference vector
 - 5: **for** $i = 1$ to b **do**
 - 6: $g_{i,t} \leftarrow \nabla_{\theta_t} \ell(s_i)$ ▷ Per-sample gradient
 - 7: $m_{i,t} \leftarrow \frac{\langle -g_{i,t}, v_t \rangle}{\|v_t\|}$ ▷ Mimic score
 - 8: **end for**
 - 9: $\bar{m}_{:,t} \leftarrow \frac{\exp(m_{:,t}/\tau)}{\sum_{j=1}^b \exp(m_{j,t}/\tau)}$ ▷ Normalize mimic scores
 - 10: $\theta_{t+1} \leftarrow \theta_t - \eta \sum_{i=1}^b \bar{m}_{i,t} \cdot g_{i,t}$ ▷ Update weights with reweighted gradients
 - 11: **end for**
-

Algorithm 2 Offline Sample Selection (Stage 2)

Input: Normalized mimic score matrix $\bar{M} = \{\bar{m}_{i,t}\} \in \mathbb{R}^{n \times T}$, binarization method `method` $\in \{\text{threshold, clustering, top-k percent}\}$, batch size b (from Stage-1)

Output: Aggregated retain probabilities p_i for each sample i , retained subset \mathcal{S}

- 1: Initialize binary decision matrix $B \leftarrow \mathbf{0}^{n \times T}$
- 2: **for** $t = 1$ to T **do**
- 3: $m \leftarrow \bar{M}_{:,t}$ ▷ Normalized mimic scores at step t
- 4: **if** `method` = `threshold` **then**
- 5: $\tau \leftarrow 1/b$ ▷ Threshold based on batch size
- 6: $B_{:,t} \leftarrow \mathbf{1}[m > \tau]$
- 7: **else if** `method` = `clustering` **then**
- 8: Fit a two-cluster k -means model on m ▷ 1D clustering
- 9: $B_{:,t} \leftarrow$ cluster assignments
- 10: **else if** `method` = `top-k percent` **then**
- 11: $\tau \leftarrow k$ -th percentile of m
- 12: $B_{:,t} \leftarrow \mathbf{1}[m \geq \tau]$
- 13: **end if**
- 14: **end for**
- 15: Train a Snorkel LabelModel \mathcal{LM} on B
- 16: $P \leftarrow \mathcal{LM}.\text{predict_proba}(B)$ ▷ Retain/discard probabilities, $P \in \mathbb{R}^{N \times 2}$
- 17: $p_i \leftarrow P_{i,1}$ for each sample i ▷ Extract retain probabilities
- 18: $\mathcal{S} \leftarrow \{i \mid p_i > 0.5\}$ ▷ Default threshold 0.5
- 19: **return** $\{p_i\}_{i=1}^n, \mathcal{S}$

C Experimental Details

We shift the focus from theoretical analysis and algorithm steps to empirical results. We first detail the training configurations and computational resources used in our experiments.

Misabeled Sample Detection. For the experiments of simulating mislabeled samples (Sec. 5.1), we fine-tune ViT-B/16 models pretrained on the ImageNet-21k dataset [56]. Training is conducted with a batch size of 32, a learning rate of 1e-4, and the AdamW optimizer. To ensure convergence, we set the training steps to 10 for the DTD and Flowers102 datasets and to 5 for the remaining datasets.

We evaluate Grad-Mimic across various temperature values τ (1.0, 0.9, 0.8, 0.7, 0.6, and 0.5) and report performance at $\tau = 0.5$ in the main paper (Table 1). Results for other temperature values are provided in Table 9. To simulate the reference model, we train ViT-B/16 models on noise-free versions of the datasets, using different random seeds for weight initialization. All experiments are conducted on an NVIDIA Tesla A100.

Large-scale Data Curation. For the experiments of multimodal data selection (Sec. 5.2), we follow the training protocol used in DataComp [54, 21] and train CLIP models from scratch using contrastive objective on image-caption pairs. Each model is trained for 5 epochs with a batch size of 4096. The total number of seen samples is 12.8M for the small-scale dataset and 128M for the medium-scale dataset.

We analyze different components of the reference model’s weights, specifically the final MLP layers in the image and text encoders. We evaluate Grad-Mimic’s effectiveness using temperature values τ of 0.03, 0.05, 0.07, 0.3, and 0.5. Performance is assessed across 38 diverse downstream tasks [21]. Results for $\tau = 0.5$ and $\tau = 0.05$ are reported in the main paper (Table 3), and comprehensive results are provided in Table 8. These experiments are conducted on 8 NVIDIA Tesla A100 GPUs.

D Comparing to Other Model-based Approaches

We compare Grad-Mimic with other model-based techniques, specifically reference model-based approach and influence function-based approach.

Reference Model-Based Approaches. We compare Grad-Mimic to Rho-Loss [14], a representative method that prioritizes samples based on excess loss, computed as the difference between the loss on the current model $\ell(\theta_t; s_i)$ and the loss on a pretrained reference model $\ell(\theta_{\text{ref}}; s_i)$. For a fair comparison, we simulate pretrained reference

	DTD			Flowers102			STL10			Oxford-IIIT Pet			CIFAR10			CIFAR100			Average		
Noise Level	0.4	0.5	0.6	0.4	0.5	0.6	0.4	0.5	0.6	0.4	0.5	0.6	0.4	0.5	0.6	0.4	0.5	0.6	0.4	0.5	0.6
Mini-Batch SGD	51.91	47.71	44.44	28.64	21.50	15.43	96.26	95.49	93.56	87.33	85.55	83.51	92.86	92.14	91.19	75.56	74.38	73.25	72.09	69.46	66.40
Rho-Loss	54.10	52.39	48.46	41.55	35.71	30.02	97.10	96.83	96.49	88.53	87.79	86.86	94.07	93.83	93.82	76.82	76.05	75.93	75.36	73.77	71.93
Grad-Mimic	54.68	54.10	50.43	42.75	37.10	31.71	97.16	97.00	96.90	88.80	88.25	87.14	94.15	93.92	93.80	77.24	76.82	76.05	75.80	74.53	73.01

Table 6: **Grad-Mimic outperforms other reference model-based methods:** Using the last-layer weights of reference model is more effective to prioritize samples for learning while reducing GPU memory usage and substantial computational overhead (see efficiency advantages are in Appendix E).

		CIFAR10	CIFAR100
Noise Level		0.5	0.5
Using full training set	Rho-Loss	93.83	76.05
	Grad-Mimic	93.92	76.82
Using hold-out training set	Rho-Loss	93.26	75.11
	Grad-Mimic	93.38	75.81

Table 7: Grad-Mimic outperforms other reference model-based methods even when using weaker or distilled reference model as proxy.

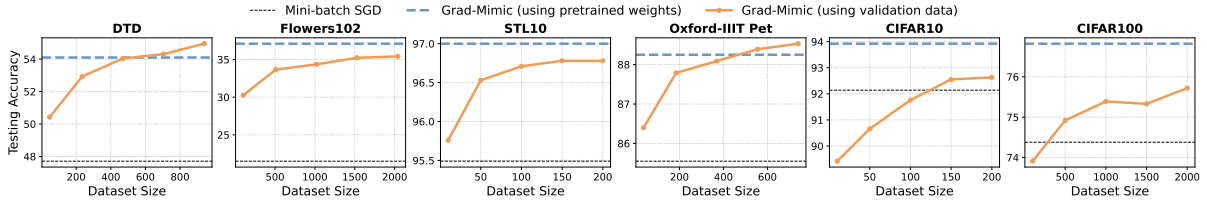


Figure 6: **Grad-Mimic outperforms approximated influence function-based methods:** Using reference model weights as selection guide offer advantages on their effectiveness and greater accessibility.

models using two approaches: (i) training on a noise-free hold-out dataset as used in Rho-Loss [14], and (ii) training on the entire training dataset, consistent with our setup in the main paper. We adopt our mislabeled sample detection setup and evaluate the model performance on the testing datasets.

We first demonstrate model performance using reference model that is trained on entire training dataset. As shown in Table 6, Grad-Mimic consistently outperforms Rho-Loss across all datasets and noise levels. Next, we benchmark both methods on CIFAR10 and CIFAR100 with 50% label noise, using a reference model trained on a noise-free hold-out dataset. Such setup simulates more realistic scenarios where the reference model, *acting as a distilled or weaker approximation of ideal weights, is used*. The results, presented in Table 7, again show that Grad-Mimic achieves higher test accuracy than Rho-Loss.

Moreover, Grad-Mimic offers other computational advantages. Unlike Rho-Loss, which requires loading the entire reference model and performing additional inference passes to compute excess loss, Grad-Mimic scores sample utility directly from discrepancies in model weights—a simpler and more efficient operation. Overall, these results are showing that *using only a subset of weights, such as those in the last layer, is sufficient for Grad-Mimic to ensure high performance, further reducing memory usage and improving computational efficiency*.

Influence Function-based Approaches. Data influence functions provide a principled way to evaluating the impact of individual training samples on model parameters [57, 58, 59], but their computational cost often limits practical use. Recent studies have explored efficient approximations that estimate sample influence by measuring gradient alignment with a noisy-free validation dataset [19, 20, 18]. We adapt these methods within Grad-Mimic framework by replacing the vector induced by reference model’s weights (v_t) with *gradients computed from a noise-free validation dataset*. We evaluate these adaptations on six image datasets by adding 50% label noise and assess the impact of validation set size by varying the number of samples drawn from per class (1, 5, 10, 15, and 20).

Results in Figure 6 show that while larger validation sets enhance data efficiency by enabling models to focus on influential samples, Grad-Mimic, which leverages pretrained reference weights and their induced direction, consistently outperforms influence approximations based on validation datasets. Moreover, relying on labeled validation sets introduces dataset dependencies, incur computational overhead from validation dataset’s gradient

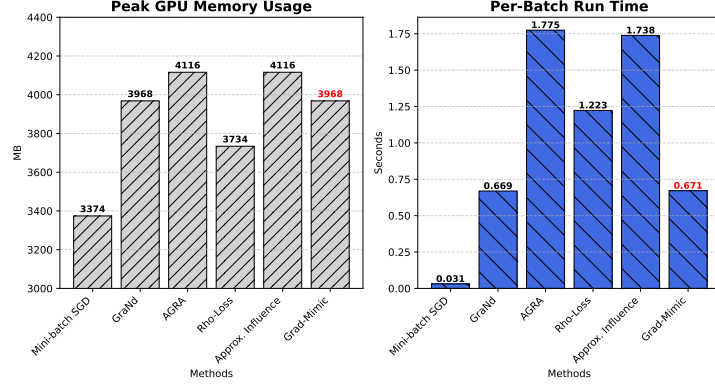


Figure 7: Grad-Mimic enjoys lower runtime per batch and smaller memory usage than other baselines.

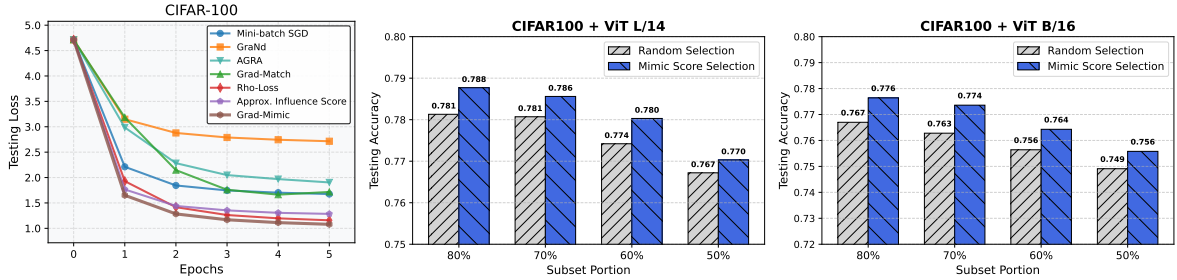


Figure 8: Grad-Mimic leads to faster convergence and improved data utilization.

computations, and poses challenges in ensuring their quality, as noted in the limitations of GREATS [18]. For example, in the out-of-domain Flowers102 dataset, achieving satisfactory performance required over 2,000 correctly labeled validation samples—*yet still fell short of Grad-Mimic’s results*.

E Efficiency Advantages

We provide four distinct lines of evidence for the efficiency gains our technique. They are (i) computational efficiency, (ii) memory usage, (iii) learning efficiency, and (iv) data utilization.

Computational Efficiency and Memory Usage. First, we benchmark *per-batch training runtime* and *peak GPU memory consumption* across considered baselines, as presented in Figure 7. Grad-Mimic achieves computational runtime and memory usage comparable to GraNd, relying solely on per-sample training gradients. In contrast, methods like AGRA and approximated influence function-based approaches incur higher computational costs due to additional gradient computations from either another training batch or a noise-free validation dataset. This creates a **2.6 times overhead**. Similarly, Grad-Mimic outperforms Rho-Loss in efficiency, as Rho-Loss requires loading a full reference model and performing additional forward passes—*substantially increasing compute time*. Regarding memory usage, Rho-Loss can exceed all these methods if the reference model size scales significantly.

Learning Efficiency. Second, we evaluate learning efficiency by analyzing convergence curves. As shown in Figure 8 (left), experiments on CIFAR100 with 50% label noise demonstrate that Grad-Mimic converges faster than all compared methods, achieving higher model performance within a fixed number of training epochs. Additionally, Figure 4 (left) illustrates that, on the DataComp medium-scale dataset (over 100 million samples), Grad-Mimic, aided by a reference model, converges faster than standard training, **reducing training steps by 20.7%**.

Data Utilization. Finally, we introduce *a new experiment* that measures data efficiency without adding label noise. Instead of simulating mislabeled samples for denoising, we rank *clean training samples* by their mimic scores and build subsets from the top-k% entries. We use a well-trained ViT-B/16 as our reference model and perform Grad-Mimic on clean CIFAR100 set. We evaluate the model performance trained on refined subsets. Results, presented in Figure 8, show that Grad-Mimic’s selected subsets consistently outperform randomly drawn subsets of the same size. Remarkably, with both ViT-B/16 and the larger ViT-L/14, Grad-Mimic **matches the full-dataset accuracy while reducing the training data by 20%**. This highlights a direct reduction in data-related computational

Scale	Training Method	Mimic Layer θ_{ref}	Temperature τ	ImageNet	ImageNet dist. shifts	VTAB	Retrieval	Average over 38 datasets (\uparrow)
Small	Vanilla Training	—	—	0.026	0.035	0.139	0.114	0.131
	Grad-Mimic	Last MLP Layer in Text Encoder	0.03	0.026	0.035	0.153	0.115	0.136
			0.05	0.026	0.035	0.147	0.114	0.135
			0.07	0.026	0.035	0.151	0.116	0.135
			0.3	0.026	0.034	0.154	0.112	0.137
			0.5	0.027	0.035	0.152	0.114	0.139
	Grad-Mimic	Last MLP Layer in Image Encoder	0.03	0.025	0.035	0.149	0.114	0.133
			0.05	0.026	0.037	0.162	0.118	0.146
			0.07	0.027	0.036	0.166	0.118	0.145
			0.3	0.026	0.035	0.161	0.114	0.144
			0.5	0.027	0.035	0.160	0.117	0.145
Medium	Vanilla Training	—	—	0.171	0.148	0.253	0.217	0.254
	Grad-Mimic	Last MLP Layer in Image Encoder	0.05	0.169	0.151	0.262	0.216	0.258

Table 8: **Full Stage 1 Results in DataComp Experiment:** On both dataset scales, with the aid of publicly available pretrained weights, Grad-Mimic consistently improves CLIP model performance across all temperature settings.

	Temperature τ	DTD	Flower102	Oxford-IIIT Pet	CIFAR10	CIFAR100
Mini-Batch SGD	—	52.8	35.6	87.9	93.2	76.2
Grad-Match	—	53.1	32.1	87.4	93.0	76.1
Grad-Mimic	1.0	56.5	44.9	89.0	94.1	77.0
	0.9	56.4	45.3	89.1	94.1	77.1
	0.8	56.3	45.8	89.1	94.1	77.2
	0.7	56.3	46.1	89.2	94.2	77.2
	0.6	56.0	46.4	89.3	94.2	77.3

Table 9: **Stage 1 Results in Simulation Experiment using Various Temperature:** Lower temperature makes the model focus more on training with high-value samples, resulting in a higher testing accuracy.

	DTD	Oxford-IIIT Pet	CIFAR10	CIFAR100
Layer 7	0.575	0.755	0.907	0.752
Layer 8	0.583	0.755	0.908	0.753
Layer 9	0.586	0.740	0.911	0.749
Layer 10	0.582	0.751	0.902	0.753
Layer 11 (last-layer weights)	0.595	0.758	0.912	0.755

Table 10: Last-layer weights yields the best performance across all datasets.

cost.

These findings—*lower runtime per batch, reduced memory usage, faster convergence, and improved data utilization*—demonstrate that Grad-Mimic achieves significant efficiency gains, fulfilling our motivation.

F Ablation Studies

Choice of Temperature. We run Grad-Mimic under different temperature values and compare them to baseline methods (Mini-batch SGD and Grad-Match [29]). The results in the simulation experiments are presented in Table 9. In these datasets, we set the noise level to 0.3 and fine-tune ViT-B/16 model under linear probing configuration. Grad-Mimic outperforms both baseline methods *at every temperature*. Lower temperatures yield better testing accuracy, as they normalize mimic scores in the way that encourages the model to focus more on high-value samples during training.

Which layer should be mimicked? Next, we study the impact of the layer weights to mimic. We vary the depth of the reference model weights used to obtain the target vector and evaluated the resulting model performance. Results,

Scale	# of samples to train θ_{ref}	Training Method	ImageNet	ImageNet dist. shifts	VTAB	Retrieval	Average over 38 datasets (\uparrow)
Small	Using 1.3B samples	Vanilla Training	0.026	0.035	0.139	0.114	0.131
	Using 1.3B samples	Grad-Mimic	0.026	0.037	0.162	0.118	0.146
	Using 3.5M samples	Grad-Mimic	0.026	0.035	0.158	0.115	0.140

Table 11: Grad-Mimic achieves performance gains even when using a weaker reference model.

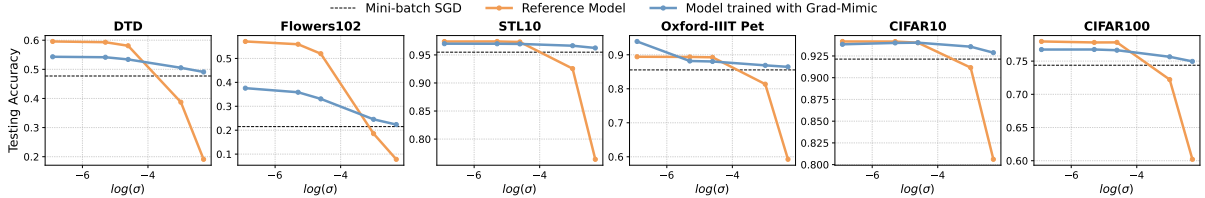


Figure 9: Grad-Mimic can be robust to the quality of reference model.

presented in the Table 10, indicate that mimicking the last-layer weights yields the highest accuracy in most cases. While the optimal choice may depend on architecture or task, these findings suggest that *later representations* generally offer the richest information and are better choices for estimating sample utility.

Impact of Reference Model Quality. Finally, we investigate how the quality of the reference model impacts the effectiveness of Grad-Mimic, particularly in scenarios where *only a weaker or distilled model is available*. To simulate such scenarios, we degrade the reference model in two controlled ways:

- **Weight corruption:** we inject zero-mean Gaussian noise ($0, \sigma^2$) into the reference model’s weights. By varying the variance of the added noise, we analyze the performance of models trained with Grad-Mimic against standard training methods that do not leverage a reference model.
- **Data-limited training:** we train the reference model on progressively smaller fractions of its original dataset (shrinking from 1.3B samples to 3.5M samples). Fewer training samples will produce a weaker (or distilled) reference model.

We assess Grad-Mimic in both the mislabeled-sample and multimodal settings, applying each degradation method separately.

We present these two analysis in Figure 9 and Table 11. As expected, increasing noise variance or using less training data degrades the reference model’s performance, which in turn lowers the effectiveness of Grad-Mimic. However, we observe that even under significant noise (heavy degradation), models trained with Grad-Mimic still outperform Mini-batch SGD and can even surpass the performance of the noisy reference model itself (see Figure 9). This highlights that *while a high-quality reference model is ideal, a weaker proxy can still provide valuable guidance and improve training over traditional baselines*.

G Broader Impacts and Limitations

Efficient data selection is a crucial prerequisite for training multimodal models. We demonstrate Grad-Mimic’s effectiveness in identifying and removing low-value samples, which enhances data efficiency and downstream model performance. We do not foresee any direct negative social consequences from the technique itself.

However, if the reference model used to evaluate sample utility is poorly calibrated or biased, there remains a risk of refining low-quality datasets. Appendix F investigates such scenario. It shows that Grad-Mimic remains competitive even when the reference model is heavily degraded, yet some performance loss is unavoidable. We believe that practitioners can easily mitigate this risk by validating the reference model on a small, trusted benchmark before data scoring. This check is easier than the requirements of many recent data-selection methods, which rely on noise-free validation sets. By decoupling data scoring from such hard-to-obtain resources, Grad-Mimic offers greater flexibility and control.